LUND UNIVERSITY

The Design of a One Dimensional Heat Diffusion Process

Leden, Bo

1970

Document Version:
Publisher's PDF, also known as Version of record

Link to publication

Citation for published version (APA):
Leden, B. (1970). *The Design of a One Dimensional Heat Diffusion Process*. (Research Reports TFRT-3026). Department of Automatic Control, Lund Institute of Technology (LTH).

Total number of authors:
1

General rights
Unless other specific re-use rights are stated the following general rights apply:
Copyright and moral rights for the publications made accessible in the public portal are retained by the authors and/or other copyright owners and it is a condition of accessing publications that users recognise and abide by the legal requirements associated with these rights.
• Users may download and print one copy of any publication from the public portal for the purpose of private study or research.
• You may not further distribute the material or use it for any profit-making activity or commercial gain
• You may freely distribute the URL identifying the publication in the public portal

Read more about Creative commons licenses: https://creativecommons.org/licenses/

Take down policy
If you believe that this document breaches copyright please contact us providing details, and we will remove access to the work immediately and investigate your claim.

LUND UNIVERSITY

PO Box 117
221 00 Lund
+46 46-222 00 00

THE DESIGN OF A ONE DIMENSIONAL HEAT DIFFUSION PROCESS

B. LEDEN

REPORT 7010 DECEMBER 1970
LUND INSTITUTE OF TECHNOLOGY
DIVISION OF AUTOMATIC CONTROL

THE DESIGN OF A ONE DIMENSIONAL HEAT DIFFUSION PROCESS.

B. Leden

ABSTRACT.

This report presents the construction of a thermal process including the electronics required to perform measurement and control the process. The control domain of the temperature is 20°C - 30°C. The thermal process has an almost unidirectional flow of heat. The influence of the environment on the stationary temperature distribution is analysed in detail. At an ambient temperature of 25°C the influence maximally reaches 0.02°C. Further a swift and stable temperature servo is developed. The servo makes use of the Peltier effect. The solution time (5% of final value) at a 2°C temperature change in the input variable is 5 sec. The long term stability (12 hours) falls below 0.001°C. The complete scheme of a cascade compensation of the servo is given. The dynamics of the process are discussed.

TABLE OF CONTENTS

1. INTRODUCTION.

The constructed laboratory process will allow experimental studies of a one dimensional heat diffusion process tied to a process computer. Problems on identifying and controlling multivariable and infinite order systems will be considered. The process will be studied mainly from two different aspects, viz. the identification and the state reconstruction and control aspects.

(i) The identification aspect:

The conduction of heat in a one dimensional heat diffusion process is well described by the partial differential equation

$$\partial^2 u/\partial x^2 - \frac{1}{a^2}\,\partial u/\partial t = 0$$

The variable $u = u(x,t)$ denotes the temperature in the process at a point x at time t. This equation may be transformed into an infinite dimensional system of ordinary differential equations. From this aspect the identification experiments are interesting. The identification results may be compared with the á priori known model.

(ii) The state reconstruction and control aspect:

The state reconstruction problem consists of the determination of the temperature profile out of an optimum mixture of mathematical model calculations on line and measurement on line. Out of the knowledge of the actual profile, the temperature profile should be controlled in an optimum way, to a desired profile by means of the controllable boundary temperatures. Among other things linear quadratic control theory will be applied. The study includes numerical methods for optimization with a process computer as well as measurement and filtering problems.

The system configuration appears in chapter 2. A brief description of the blocks forming the system and the system requirements are also presented here. The requirements are the ones satisfied by the system. Thus the performance figures of the system may readily be found.

Chapter 3 deals with the construction of a swift and stable temperature servo, making use of the Peltier effect. The servo comprises a PID regulator and a nonlinear compensation, introduced in the feedforward path. The step responses of the servo to a temperature change of $\pm 1^{\circ}C$, $\pm 2^{\circ}C$, and $\pm 4^{\circ}C$ are shown in Fig. 3.4.4. The effect of the saturation obtained in the servo may be studied from those figures. The transient response in 3 different points of the servo is found in Fig. 3.4.2 and 3.4.3. The figures show clearly the effect of the nonlinear compensation. The solution time (5% of final value) of the servo reaches 5 sec. at a $2^{\circ}C$ step change in the input variable.

We are concerned with the problem of insulation in chapter 4. The temperature distribution in a thin rod is evaluated on the assumption, that the thermal losses from each surface element are proportional to the temperature difference between the environment and the element. As a consequence of the evaluation we conclude, that the system requirements cannot be fulfilled, provided that a conventional insulation technique is employed. A solution to the problem is achieved by enclosing the rod in a heat shield controlled as the rod. A detailed analysis of the stationary temperature distribution of the process is carried out.

In chapter 5, finally, the dynamics of the process and the measurement results are presented. A modal analysis shows, that the transfer function between the end point temperature and the temperature at an arbitrary point on the rod contains an infinite number of negative real poles. The unit step responses of the process are calculated and appear in Fig. 5.1.3. The measurement results are shown in sections 5.3.2 and 5.3.3. Section 5.3.2 treats the stationary case. The temperature distribution of the

rod at different boundary temperatures may be studied from Tables 5.2.1 and 5.2.2. The control domain of the temperature is $20^{\circ}C$ - - $30^{\circ}C$. In the domain the influence of the environment on the temperature distribution maximally reaches $0.02^{\circ}C$, provided that the ambient temperature is $25^{\circ}C$. Section 5.3.3 considers the nonstationary case. The influence of the environment and the servo on the step responses of the process may be studied from Fig. 5.3.1 and 5.3.2. The influence rapidly decreases as the measuring point is removed from the excitation point. In the reduced temperature range $24^{\circ}C$ - $26^{\circ}C$ the influence falls below $0.003^{\circ}C$ for $x \geq \ell/2$.

2. A GENERAL DESCRIPTION OF THE SYSTEM.

2.1. A Block Diagram of the System.

The system configuration is shown in the block diagram, Fig. 2.1.1.

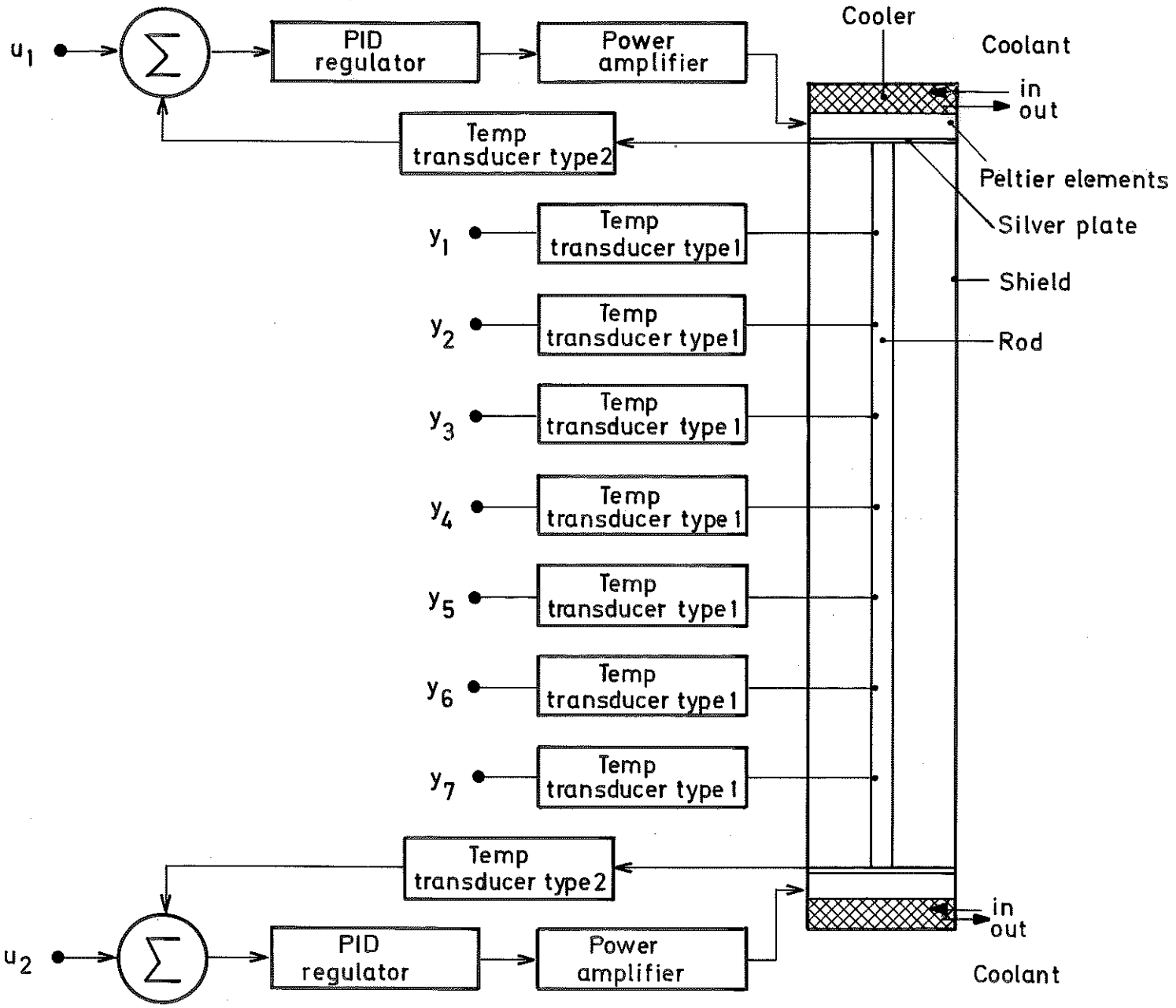

Fig. 2.1.1 - A block diagram of the system.

The diagram shows that the system comprises a thermal process, 7 temperature transducers and 2 servo loops, forming so-called temperature servos. The system input variables are u_1 and u_2, and the system output variables y_1, y_2 ... y_7.

The thermal process is made of a straight homogeneous copper rod with constant cross section. The rod is enclosed in a copper shield. The shield yields an almost unidirectional flow of heat in the rod. A conventional heat insulation surrounds the shield. The silver plate connects thermally the end surfaces of the rod and the shield. The Peltier elements, connected to the silver plate, supply the power necessary to control the end temperature of the rod. The coolant serves as a reference temperature to the Peltier elements. The rod has 9 equal spaced small holes. Two holes are situated in the end surfaces and 7 along the rod. A sensor can be mounted in each hole.

The transducers are of two types. The connection between the body temperature $T^{o}C$ of the sensor and the output voltage e volts of the transducer is

$$e = \pm(25 + T) \qquad (2.1.1)$$

where the plus sign applies for type 1 and the minus sign for type 2. The temperature range of operation is $20^{o}C$ - $30^{o}C$. The output voltages of the transducers type 1 are the output variables of the process denoted y_1, y_2, y_3 ... y_7 in the block diagram. The transducer type 2 is used in the servo loops. The voltage-temperature characteristic of the transducers are shown in Fig. 2.1.2.

The servo loops include 5 blocks, one of which is the transducer type 2. The other blocks are a summing amplifier, a PID regulator, a power amplifier, and the Peltier elements with cooler. The end temperatures of the rod are controlled by means of the system input variables u_1 and u_2. An input signal u volts yields the stationary end temperature $T^{o}C$ where

$$T = (u + 25) \qquad (2.1.2)$$

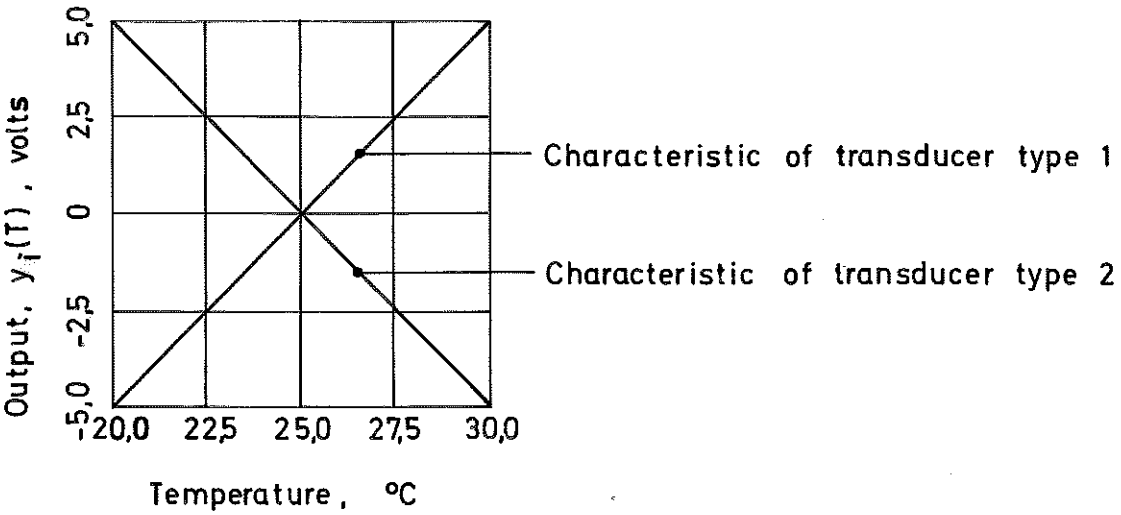

Fig. 2.1.2 - The voltage-temperature characteristic of the temperature transducer type 1 and type 2. Temperature range $20^{\circ}C$ - $30^{\circ}C$.
The sensing element of the transducer is a thermistor.

2.2. A Summary of the Different Blocks.

The temperature transducer consists of a one thermistor Wheatstone bridge and a differential amplifier. The amplifier detects the unbalance of the bridge, which is fed by a stable reference voltage. The linearity error of the transducer reaches $0.01^{\circ}C$ in the temperature range $20^{\circ}C$ - $30^{\circ}C$. A detailed description of the transducer is found in |3|. The summing amplifier has two inputs and is inverting. The PID regulator is made up of a serie connection of an integrating compensation and a lead compensation. The regulator contains a compensation for the nonlinearity of the Peltier elements. The power amplifier supplies a maximum direct current power of 130 watts at the resistive load 1 ohm. The power is limited by the PID regulator to 80 watts. The gain of the amplifier is 10 times. The Peltier elements generate a maximum cooling effect of 46 watts. The maximum heating effect is essential-

ly greater but is limited by the regulator to 46 watts. The magnitude and direction of the current supplied to the elements control the magnitude and direction of the flow of heat through the elements. A more detailed description of the summing amplifier, the PID regulator, the power amplifier and the Peltier elements appears in section 3.2., 3.3 and 3.4.

2.3. System Requirements.

In the introduction it was mentioned, that the constructed thermal process was intended to allow experimental studies of a one dimensional heat diffusion process, tied to a process computer. It was also stated, that the process should be studied from mainly the identification and the state reconstruction and control aspect. Some experiments, especially the identification experiments, require that a quite accurate realization of the one dimensional heat diffusion process is available. However, it has not been possible to obtain a precise bound for the influence of the environment and the servos on the measured performance of the process. The philosophy has been to build the process as accurately as possible with a reasonable amount of effort. The requirements below are fulfilled by the system and are the measured performance figures. It should also be pointed out, that the conduction of heat in a real specimen with a unidirectional flow of heat is not perfectly described by the one dimensional heat diffusion equation. The accuracy of a physical realization of this equation is thus limited.

The control domain of the temperature is $20^{\circ}C$ - $30^{\circ}C$. In this domain we now specify at an ambient temperature of $25^{\circ}C$.

Heat insulation:

(i) The influence of the environment upon the steady state temperature distribution of the rod should be within $0.02^{\circ}C$.

Transducer:

(ii) The linearity error of the transducer must be below $0.02^{\circ}C$.

(iii) The drift (12 hours) of the transducer must be within $0.001^{\circ}C$.

(iv) The short time stability (1 min.) of the transducer should fall below $0.0002^{\circ}C$.

Servo:

(v) The stationary error of the servo must be below $0.01^{\circ}C$.

(vi) The solution time (5% of final value) of the servo to a reference temperature change of $2^{\circ}C$ must be within 5 sec.

(vii) The drift (12 hours) of the servo should fall below $0.001^{\circ}C$.

(viii) The short time stability (1 min.) of the servo should be better than $0.0002^{\circ}C$.

The extreme requirements on the drift and stability of the transducer and servo make it possible to utilize a narrower temperature range for the experiments without having the accuracy spoiled by noise and drift. This may in some cases be of great advantage as the solution time of the servo increases considerably when the input signal essentially exceeds $2^{\circ}C$. The linearity of the employed transducers is improved as the temperature range is reduced symmetrically around the mid point temperature $25^{\circ}C$.

Section 5.1 shows that at an irrational point the transfer function between the end temperature of the rod and the temperature of the irrational point contains 10 poles to the right of the control poles of the servo. Thus we conclude that the process may be properly excited. The employed transducers found in |3| fulfil specifications (ii), (iii) and (iv).

3. A TEMPERATURE SERVO.

3.1. A Block Diagram of the Servo.

The block diagram of the servo is presented in Fig. 3.1.1.

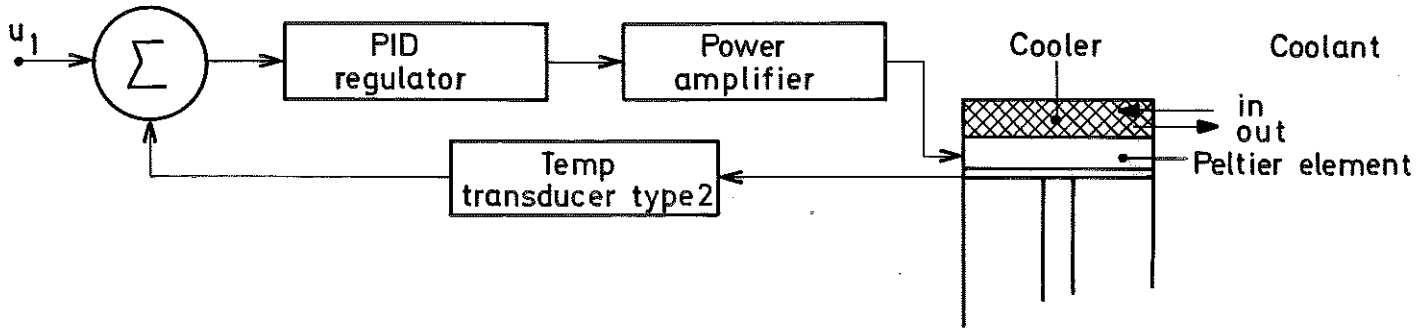

Fig. 3.1.1 - The block diagram of the servo.

The servo comprises 5 blocks. The open loop system is formed by the serie connection of the power amplifier, the Peltier elements, and the transducer. The input and output variables of the open system are the input signal of the power amplifier and the output signal of the transducer respectively. The open system is approximately linear as small input signal amplitudes appear. The Bode plots of the uncompensated and the compensated system are shown in Fig. 3.1.2. The PID regulator, placed in the feedforward path, is a serie compensation. The compensation yields an improved swiftness and stability of the servo, and reduces the static error to zero.

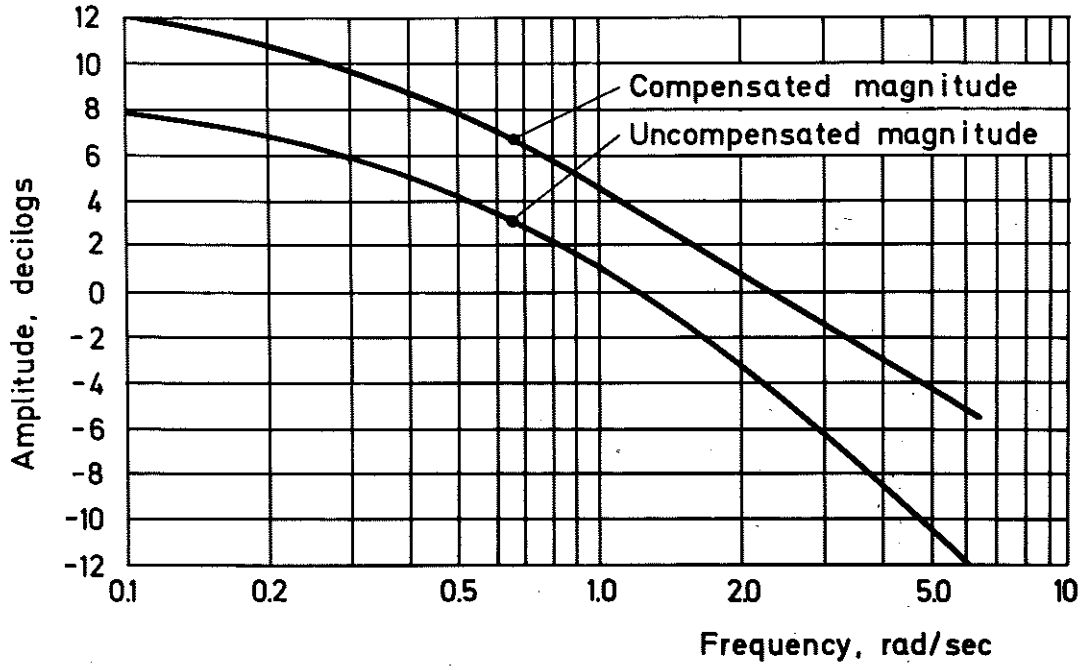

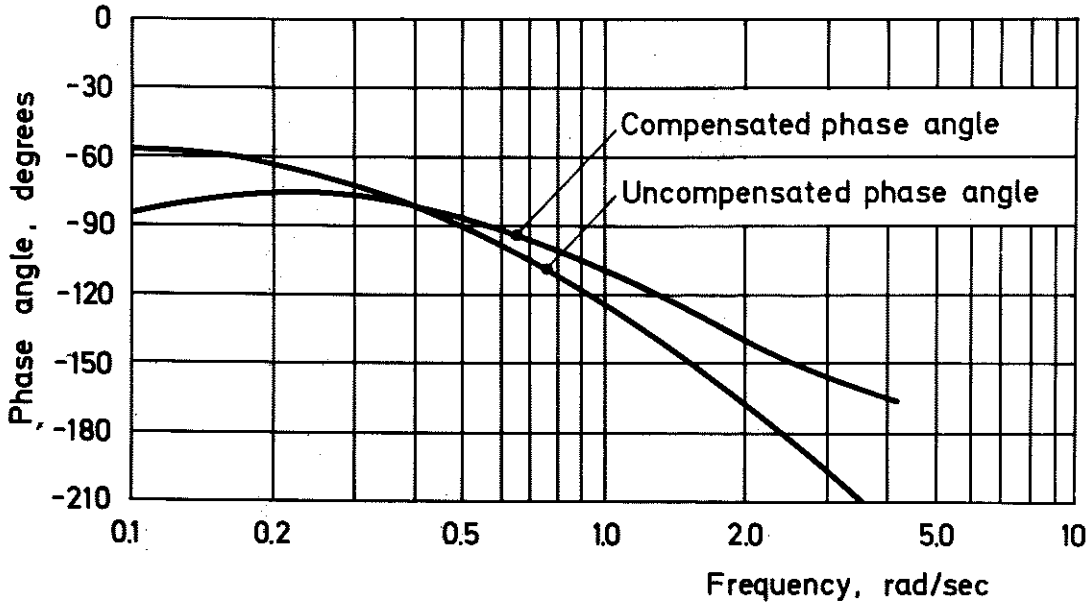

Fig. 3.1.2 - The Bode diagrams of the uncompensated and the compensated system.

3.2. A Design Criterion of the PID Regulator.

The PID regulator consists of a cascade connection of an integrating compensation $(1 + 1/Ts)$ and a lead compensation $K(s + b)/(s + bN)$.

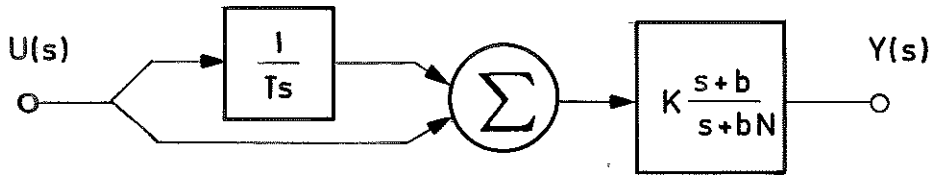

Fig. 3.2.1 - The block diagram of PID regulator.

The transfer function of the compensation is

$$K(1 + 1/Ts)\,\frac{s + b}{s + bN} \qquad (3.2.1)$$

The integrating compensation reduces the static error coefficient to zero, required by the system requirement (v).The parameters K, T, b and N should be determined, e.g. from the Bode diagram of the open loop system, to give the servo an optimum transient behaviour and a solution time below 5 sec. The parameter b is chosen to make crossover occur within a long section of -20 dB per decade slope. This insures an adequate phase margin. The phase margin may be increased or decreased by adjusting K.

As a rule of thumb the parameter T should be chosen to make the integrating compensation cause a phase lag of 5° at crossover. Such a choice affects only the stability of the closed loop system slightly and yields a static error quickly tending to zero.

The lead compensation improves the transient behaviour of the system by giving a positive phase shift at crossover. The maximal phase-lead angle obtained by the compensation is

$$\phi_{max} = \text{arctg}\{(\sqrt{N} - 1/\sqrt{N})/2\} \qquad (3.2.2)$$

and occurs at the angular frequency $b\sqrt{N}$. The limiting phase-lead angle of eq. (3.2.2) is 90°. Clearly, the angle readily obtainable from the compensation is not much greater than 60°. The choice N = 10, which prevents the feedforward path to become too susceptible to noise, often appears in practice.

The rules of thumb presented above suggest

$$\begin{cases} K = 24 \\ 1/T = 0.053 \\ b = 3.12 \\ N = 11 \end{cases} \qquad (3.2.3)$$

The K value gives the compensated system the phase margin 35°. The choice of T results in a phase lag of 1.4° at crossover. Further, the choices of b and N give a phase-lead angle of 33° at crossover. According to eq. (3.2.2) a maximum phase-lead angle of 56° may be obtained, provided that the frequency $b\sqrt{N}$ equals the crossover frequency. This suggests a larger b value. In practice the chosen b value is found "optimum". The discrepancy may be caused by the rapid phase angle decrease at crossover.

The bandwith of the system is 4.1 rad/sec. From Fig. 3.4.4 it appears, that the solution time (5% of final value) of the servo is 5 sec. at a 2°C change in the reference temperature. The system requirement (vi) is thus satisfied.

3.3. A Design of a PID Regulator.

The integrating compensation is realized with the circuit 3.3.1.

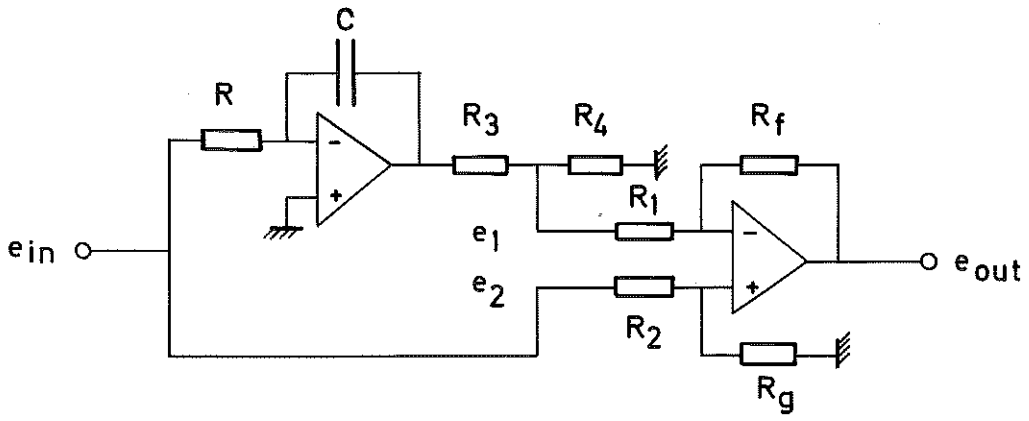

Fig. 3.3.1 - The realization of the integrating compensation.

The compensation contains an integrator and a differential amplifier. The integrator is connected to the differential amplifier via a voltage divider. This provides an artificial increase of the characteristic time RC of the compensation. A realization of the compensation involving one operational amplifier is readily found for time constants T of the order of 1 sec.

Provided, that the loading effect of R_1 on R_3 and R_4 is negligible, i.e.

$$R_1 >> R_3//R_4 \tag{3.3.1}$$

the following relations between the voltages e_1, e_2, e_{in}, and e_{out} hold

$$e_{out} = -\frac{R_f}{R_1} e_1 + \frac{1 + R_f/R_1}{1 + R_g/R_2} e_2 \tag{3.3.2}$$

$$e_1 = - \frac{R_4}{R_3 + R_4} \frac{1}{RC} \int e_{in}\, dt \qquad (3.3.3)$$

It should be observed that $e_2 = e_{in}$. The transfer function $G_{cl}(s)$ of the circuit is readily obtained by substituting eq. (3.3.3) into (3.3.2) and making a Laplace transformation. The procedure yields

$$G_{cl}(s) = \frac{1 + R_f/R_1}{1 + R_g/R_2} \left(1 + \frac{R_f}{R_1} \frac{R_4}{R_3 + R_4} \frac{1 + R_g/R_2}{1 + R_f/R_1} \frac{1}{RC} \frac{1}{s} \right) \qquad (3.3.4)$$

By introducing the gain factor K_1 and the time constant T the transfer function may be written

$$K_1(1 + 1/Ts) \qquad (3.3.5)$$

where

$$K_1 = \frac{1 + R_f/R_1}{1 + R_g/R_2} \qquad (3.3.6)$$

$$1/T = \frac{R_f}{R} \frac{R_4}{R_3 + R_4} \frac{1 + R_g/R_2}{1 + R_f/R_1} \frac{1}{RC} \qquad (3.3.7)$$

In the previous section the parameter T was determined. We have

$$1/T = 0.053 \qquad (3.3.8)$$

The time constant T is thus 19 sec. The nonlinear compensation, described later, requires a gain factor K_1 of approximately 5.

We now rather arbitrary put

$$\begin{cases} R = 390\ k\Omega \\ C = 6.8\ \mu F \\ R_1 = R_2 = R_g = 39\ k\Omega \\ R_3 = 8.3\ k\Omega \\ R_f = 400\ k\Omega \end{cases} \qquad (3.3.9)$$

The moderate value of the resistance R will prevent the input offset current of the operational amplifier from causing damaging disturbances on the performance of the integrator. Further, the moderate value of the capacitance C allows us to find a low-leakage capacitor of small dimensions. The choices of R_1, R_2 and R_3 need no comments. The value of R_3 gives a resistance R_4, which satisfies the inequality (3.3.1). The choice of R_f is due to the requirement of the gain K_1. Combining eq. (3.3.7) and (3.3.8) we find

$$R_4 = 700\ \Omega \qquad (3.3.10)$$

Finally, we obtain from eq. (3.3.6) and (3.3.9)

$$K_1 = 5.6 \qquad (3.3.11)$$

The transfer function (3.3.5) hence is

$$5.6(1 + 0.053/s) \qquad (3.3.12)$$

The circuit diagram of the lead compensation is found in the Fig. 3.3.2.

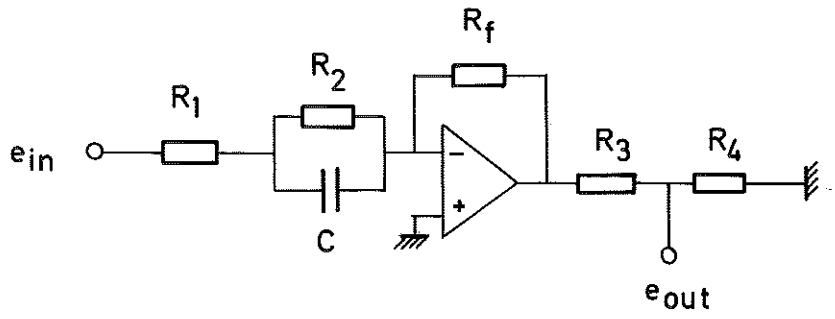

Fig. 3.3.2 - The circuit diagram of the lead compensation.

The nonlinear compensation employed requires, that the output swing of the operational amplifier is ±10 volts, while the maximum permitted input swing of the power amplifier is ±1 volt. Therefore the voltage divider should be introduced. The transfer function $G_{c2}(s)$ of the lead compensation is

$$G_{c2}(s) = - K_2 \frac{R_4}{R_3 + R_4} \frac{s + b}{s + bN} \tag{3.3.13}$$

where

$$b = 1/(R_2C) \tag{3.3.14}$$

$$N = 1 + R_2/R_1 \tag{3.3.15}$$

$$K_2 = R_f/R_1 \tag{3.3.16}$$

The parameters b and N were determined in the previous section. We found

$$\begin{cases} b = 3.12 \\ N = 11 \end{cases} \tag{3.3.17}$$

We now again rather arbitrarily choose

$$\begin{cases} R_2 = 100\ k\Omega \\ R_3 = 10\ k\Omega \\ R_4 = 1\ k\Omega \end{cases} \tag{3.3.18}$$

According to eq. (3.3.14), (3.3.15) and (3.3.17) we obtain

$$\begin{cases} C = 3.2\ \mu F \\ R_1 = 10\ k\Omega \end{cases} \tag{3.3.19}$$

It now remains to choose R_f to obtain a phase margin of 35°. As shown in section 3.2 this requirement implies

$$K = K_1 K_2 \frac{R_4}{R_3 + R_4} = 24 \tag{3.3.20}$$

This finally yields

$$R_f = 470\ k\Omega \tag{3.3.21}$$

An insertion of the parameter in the transfer function (3.3.13) gives

$$G_{c2}(s) = -\ 4.3\ \frac{s + 3.1}{s + 34} \tag{3.3.22}$$

3.4. Open Loop System, a Nonlinear Compensation and Transient Performance of the Servo.

The circuit diagram of the summing amplifier is found in the complete scheme of the compensation Fig. 3.4.1 . The transfer function between either input and the output of the amplifier is

$$-\frac{1}{1+Ts}, \quad T = 0.033 \tag{3.4.1}$$

which tends to -1 for small frequencies s. The dynamics of the amplifier do not affect the transient performance of the servo, but makes it less susceptible to noise components in the input signal. The corner frequency of the transfer function is 30 rad/ /sec. The tolerance of the employed input and feedback resistances is 0.1%. The reference temperature of the servo is obtained from a stable zenerdiode bridge.

The power amplifier supplies a maximum direct current power of 130 watts at the resistive load 1 ohm. The gain is 10 times, and the input and output impedances are 500 kohms and 25 mohms respectively. The output noise (RMS) at short-circuited input and 1 ohm load is 0.3 mvolts. The cut-off frequency (-3 dB) of the amplifier is 18 kHz. The actual load is 0.8 ohms, giving a maximum power of 100 watts. The Peltier elements require the maximum power of 80 watts at an output current of 10 amp. A detailed description of the amplifier may be found in |4|.

The Peltier element is made of a semi-conductor and consists of 36 pairs of different doped small bars, joined with copper bridges. The current through the elements pump heat from one side of the element to the other side. The direction of the flow of heat is altered by a reversed current. The power transferred through the element is as a first approximation proportional to the magnitude of the current. However, the process occurs with ohmic losses.

If a constant temperature difference exists across the element the relation (4.3.2) holds

$$P = k_1 I + k_2 I^2 \qquad (4.3.2)$$

where P denotes the power, supplied by the element, and I the current through the element. The quotient k_1/k_2 is 10 - 20 amp. The maximum cooling effect is obtained at the current 10 amp at zero temperature difference across the element and reaches 23 watts. Each servo contains two Peltier elements. Thus a maximum cooling effect of 46 watts is generated.

The nonlinear compensation is found in Fig. 3.4.1. The first compensation, consisting of a single zenerdiode, is inserted across one of the feedback resistances of the differential amplifier. The compensation gives the amplifier a voltage dependent gain. In a case, where a large positive input signal is applied to the servo, the zenerdiode is forward biased, yielding a short-circuit of the feedback potentiometer. In the opposite case the diode is not active.

The second compensation is a limiter, made up of two different zenerdiodes, connected in series. The limiter is found across the feedback resistances of the lead compensation. The bounds of the output of the operational amplifier concerned become 5.6 V for a positive output and 9.3 V for a negative output. These bounds are chosen so that approximately the same maximum heating and cooling effect is obtained in the Peltier elements. The employed diodes have a steep forward characteristic, yielding a limiter with sharply-defined bounds. Note, that the limiter prevents the operational amplifier of the lead compensation from being overloaded. Also note, that small changes in the input signal never activate the nonlinear compensation, which creates a linear band in the servo.

The transient response in three different points in the servo may be seen in Fig. 3.4.2 and 3.4.3. The change in the input signal is 1 V and -1 V respectively. The effect of the nonli-

near compensation may be studied from those figures. In Fig. 3.4.4 the step responses of the servo is shown at an input voltage change of ±1 V, ±2 V and ±4 V. The solution time of the servo increases considerably when the reference input change essentially exceeds 2 V.

The maximum steady temperature difference between the servo input signals reaches 0.01°C. The drift (12 hours) of the servo is below 0.001°C and its short time stability (1 min.) is within 0.0002°C. Thus the system requirements (v), (vii) and (viii) are satisfied.

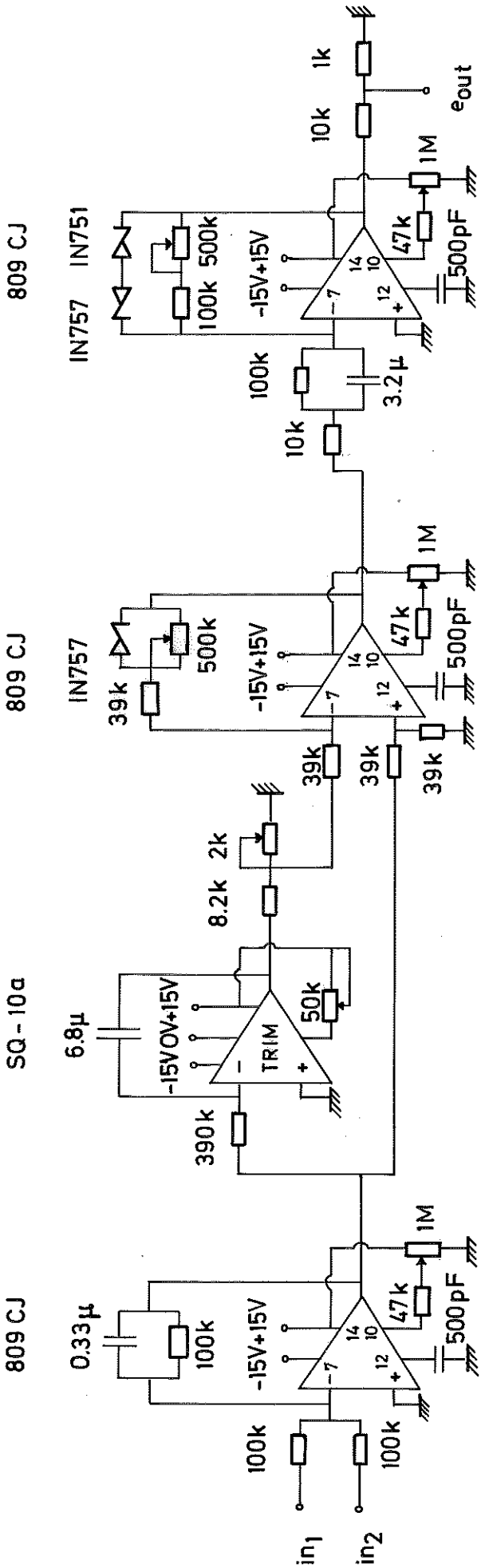

Fig. 3.4.1 - The complete scheme of the compensation.

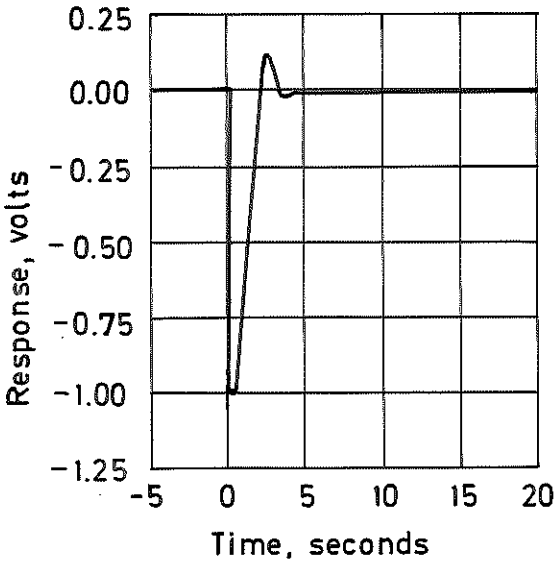

The output of the summing amplifier

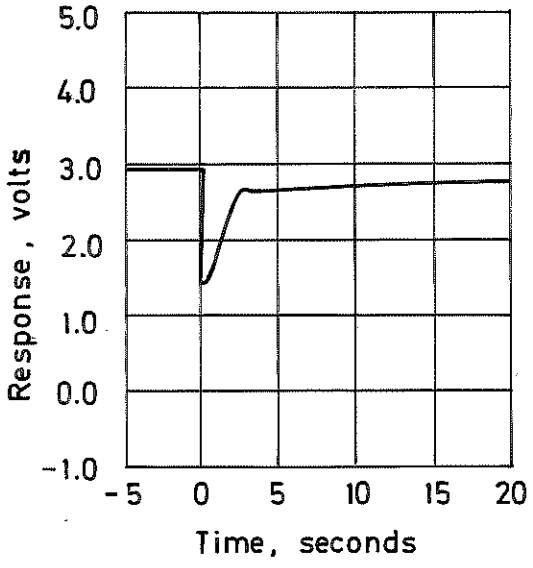

The output of the integrating compensation

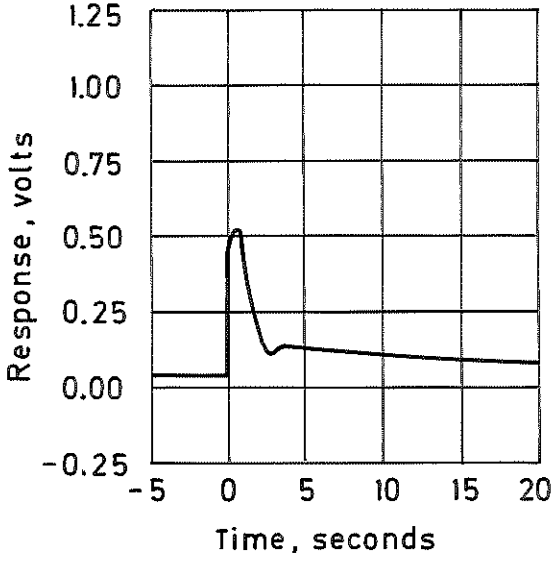

The output of the lead compensation

Fig. 3.4.2 - The transient response in three different points in the servo. Reference temperature change $1^{o}C$.

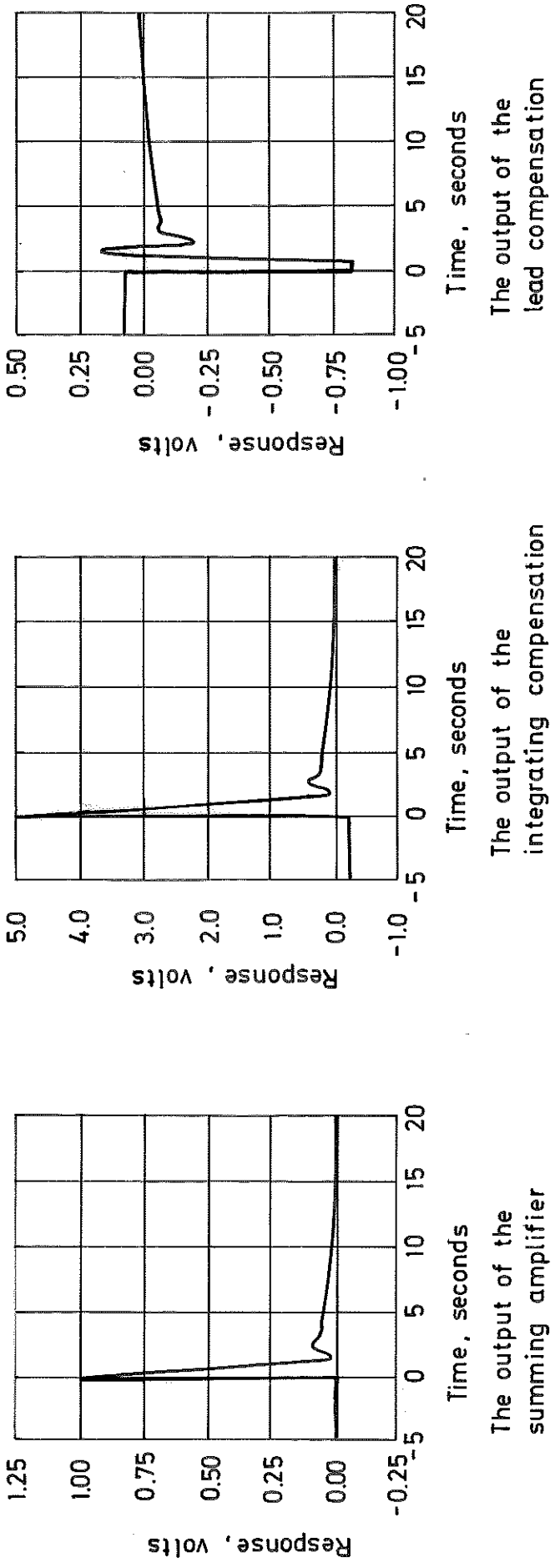

Fig. 3.4.3 - The transient response in three different points in the servo.
Reference temperature change -1°C.

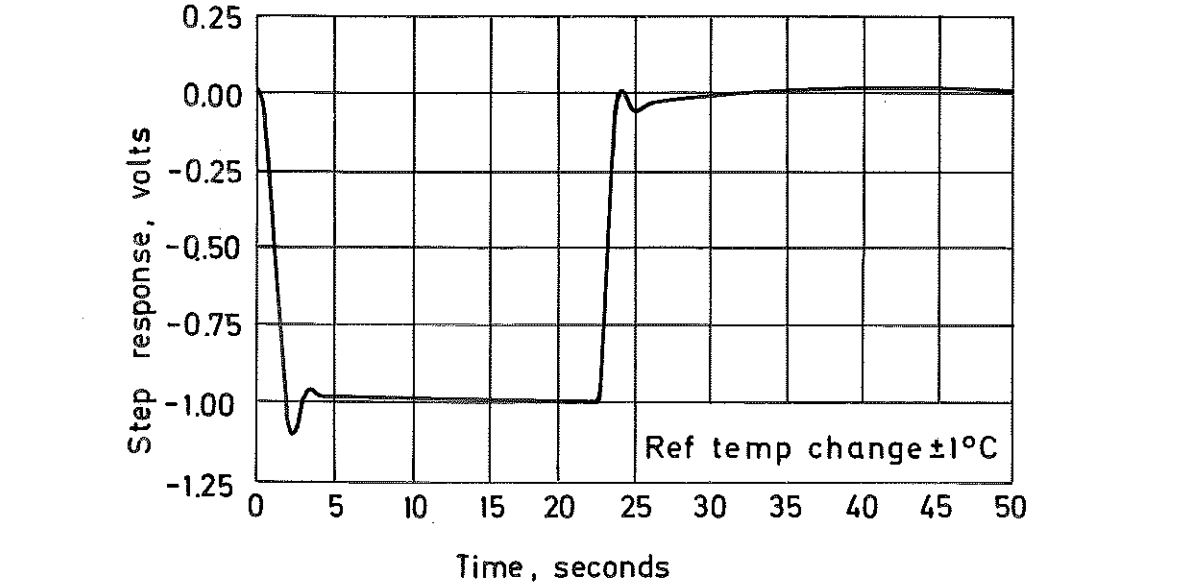

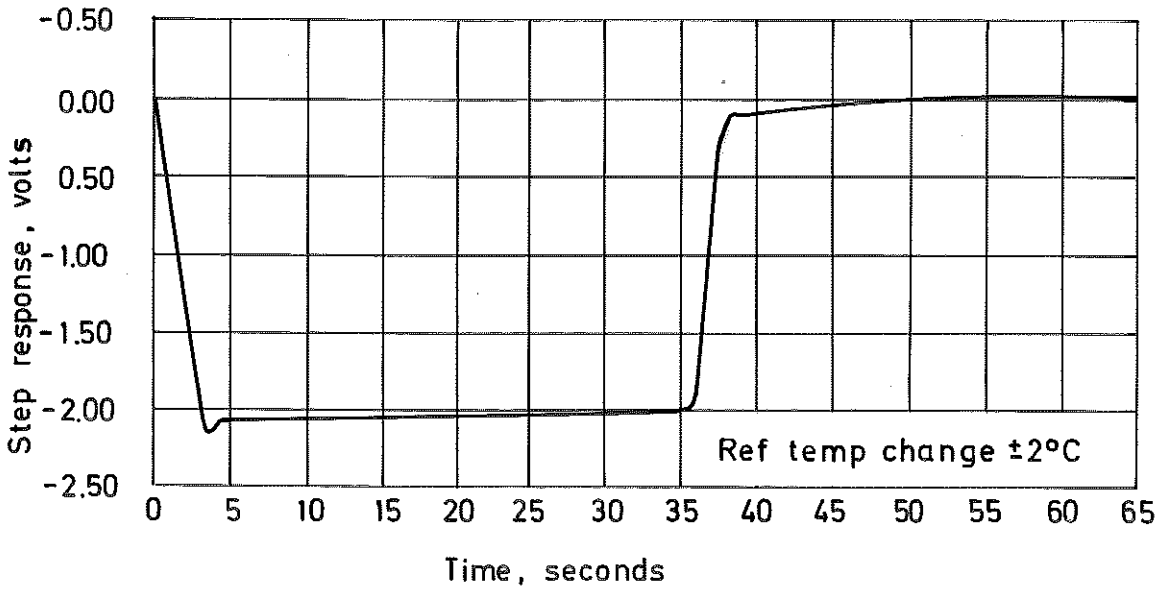

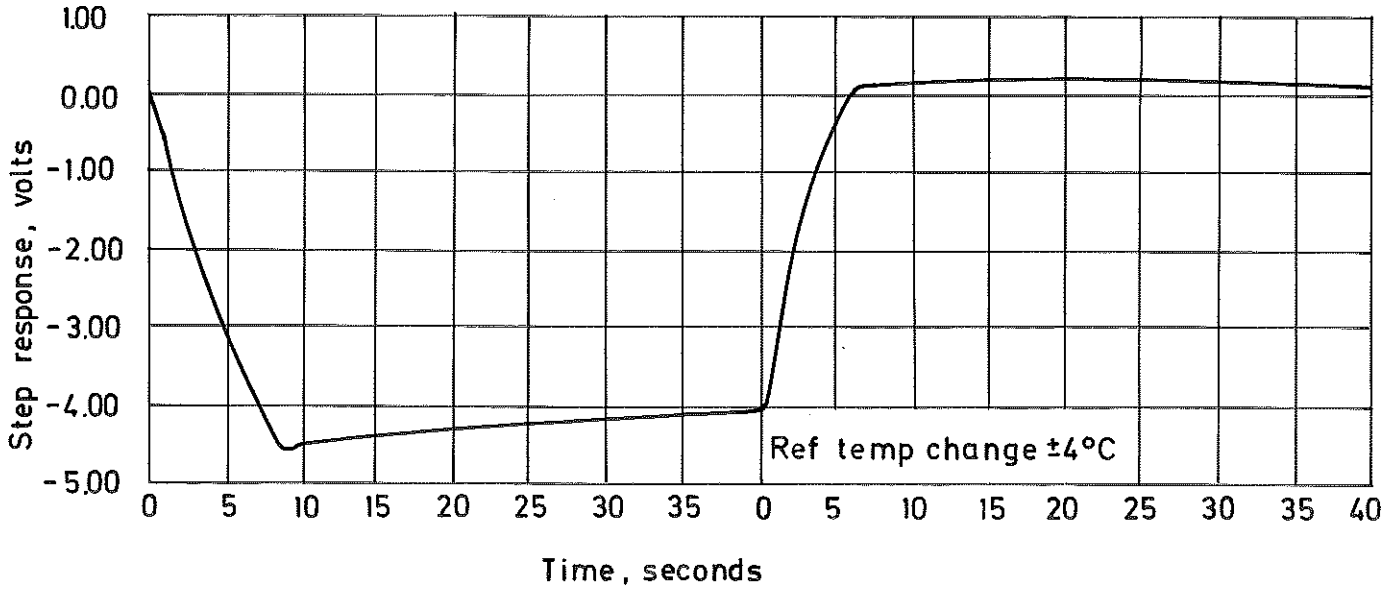

Fig. 3.4.4 - The step responses of the servo at different reference temperature changes.

4. APPROACHES TO THE PROBLEM OF INSULATION.

4.1. Fundamentals of Conduction of Heat in Solids.

In this section we are concerned with the differential equation describing the conduction of heat in an isotropic homogeneous solid. This equation turns out to be a nonlinear partial differential equation. Only in a case, where the thermal properties of the solid are independent of the temperature the well-known heat conduction equation is obtained.

Let $u = u(\bar{r},t)$ be the temperature at a point $\bar{r}$ of the solid at time t. Further, let heat be produced in the solid, so that at the point $\bar{r}$ at time t, heat is supplied at the rate $Q = Q(\bar{r},t)$ per unit time per unit volume. Denote the thermal conductivity, the density and the specific heat of the solid by k, ρ and c respectively. These quantities are functions of the temperature u. An energy balance yields

$$\rho c \frac{\partial u}{\partial t} = \frac{\partial}{\partial x}\left(k \frac{\partial u}{\partial x}\right) + \frac{\partial}{\partial y}\left(k \frac{\partial u}{\partial y}\right) + \frac{\partial}{\partial z}\left(k \frac{\partial u}{\partial z}\right) + Q \qquad (4.1.1)$$

Observing, that the thermal conductivity k depends on u, this equation becomes

$$\rho c \frac{\partial u}{\partial t} = k\left(\frac{\partial^2 u}{\partial x^2} + \frac{\partial^2 u}{\partial y^2} + \frac{\partial^2 u}{\partial z^2}\right) + Q + \frac{\partial k}{\partial u}\left(\left(\frac{\partial u}{\partial x}\right)^2 + \left(\frac{\partial u}{\partial y}\right)^2 + \left(\frac{\partial u}{\partial z}\right)^2\right) \qquad (4.1.2)$$

If the thermal conductivity k is independent of the temperature, the factor $\partial k/\partial u$ vanishes, and eq. (4.1.2) is simplified to

$$\frac{\partial^2 u}{\partial x^2} + \frac{\partial^2 u}{\partial y^2} + \frac{\partial^2 u}{\partial z^2} - \frac{\rho c}{k} \frac{\partial u}{\partial t} = - Q/k \qquad (4.1.3)$$

This is the well-known heat conduction equation. However, in general the thermal properties of the solid depend slightly on the temperature. The following expressions apply for copper in the

temperature range $20^{\circ}C$ - $30^{\circ}C$.

$$k = k_0(1 + \alpha u); \quad k_0 = 3.8 \text{ W/cm } ^{\circ}C; \quad \alpha = -3\ 10^{-4}/^{\circ}C \tag{4.1.4}$$

$$c = c_0(1 + \beta u); \quad c_0 = 0.39 \text{ J/g } ^{\circ}C; \quad \beta = 3\ 10^{-4}/^{\circ}C \tag{4.1.5}$$

$$\rho = \rho_0(1 + \gamma u); \quad \rho_0 = 8.9 \text{ g/cm}^3; \quad \gamma = -0.5\ 10^{-4}/^{\circ}C \tag{4.1.6}$$

The subscript o refers to the temperature $20^{\circ}C$.

Eq. (4.1.2) may be reduced to a simpler form by introducing the variable $\theta = \theta(\bar{r},t)$, |2|.

$$\theta = \frac{1}{k_0} \int_0^u k(\xi)d\xi \tag{4.1.7}$$

The conductivity k_0 is merely introduced to give θ the dimension of temperature and is the value of k at u = 0. Eq. (4.1.2) now becomes

$$\frac{\partial^2\theta}{\partial x^2} + \frac{\partial^2\theta}{\partial y^2} + \frac{\partial^2\theta}{\partial z^2} - \frac{\rho c}{k} \frac{\partial\theta}{\partial t} = -\frac{Q}{k_0} \tag{4.1.8}$$

where $\rho c/k$ depends on θ. The case of stationary one dimensional flow with no heat generation is of particular interest. Eq. (4.1.8) may then be written

$$\frac{d^2\theta}{dx^2} = 0 \tag{4.1.9}$$

Thus

$$\frac{d\theta}{dx} = a = \text{const} \tag{4.1.10}$$

i.e. the temperature gradient of the variable θ is constant.

From eq. (4.1.7) it follows

$$\frac{du}{dx} = \frac{k_0}{k} \frac{d\theta}{dx} \tag{4.1.11}$$

According to eq. (4.1.4) and (4.1.10) an integration of this relation yields

$$ax = u + \frac{1}{2} \alpha u^2 \tag{4.1.12}$$

For the sake of simplicity it is assumed, that the temperature at $x = 0$ is zero. Employing eq. (4.1.12) u may be expressed as a function of x. The following approximate expression is obtained.

$$u(x) = ax - \frac{1}{2} \alpha a^2 x^2 \qquad \alpha ax << 1 \tag{4.1.13}$$

The relation (4.1.13) is shown graphically in the figure below for α less than zero. This sign is applicable for copper.

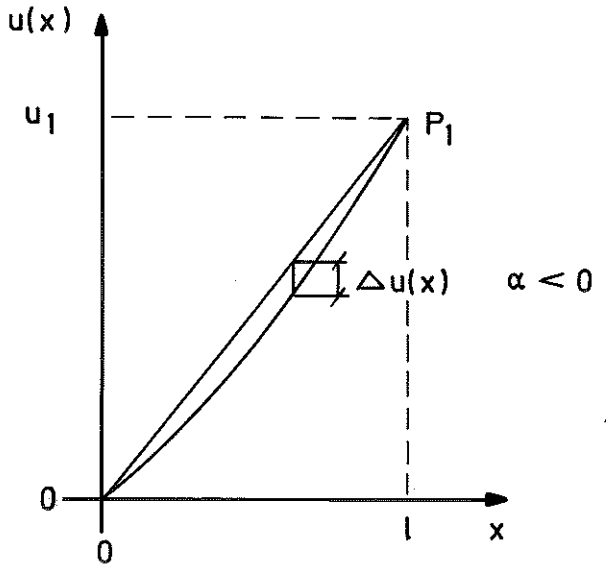

Fig. 4.1.1 - The stationary temperature gradient in an isotropic homogeneous slab.

In the figure the point P_1 and origo denote two arbitrary points, spaced at a distance ℓ from each other. The vertical distance $\Delta u(x)$ between the function (4.1.13) and the straight line is readily calculated. We obtain

$$\Delta u(x) = \frac{1}{2} \alpha a^2 x(\ell - x) \tag{4.1.14}$$

The maximum value of Δu is achieved at $x = \ell/2$ and reaches

$$\Delta u(\ell/2) = \frac{1}{8} \alpha a^2 \ell^2 \tag{4.1.15}$$

Given that the solid is copper and the temperature difference between the two points $10^{\circ}C$ we have approximately

$$a\ell = 10 \tag{4.1.16}$$

which yields according to eq. (4.1.4) and (4.1.5)

$$\Delta u(\ell/2) = 0.003^{\circ}C \tag{4.1.17}$$

We now conclude that the temperature distribution in a perfectly insulated isotropic homogeneous copper rod, whose end surfaces are kept at constant temperatures, is not linear. As illustrated in the Fig. 4.1.1, the temperature gradient in such a rod increases slightly with increasing temperature. However, defining the departure from linearity as in eq. (4.1.14) we know, that the maximum linearity error in a temperature interval of $10^{\circ}C$ only comes up to $0.003^{\circ}C$. Finally, it is mentioned, that nonstationary heat conduction in a solid, whose thermal properties are temperature dependent, is not simply handled.

4.2. A First Approach to the Problem of Insulation.

In this section we consider the conduction of heat in a rod. The quotient of the radius and the length of the rod is assumed to be so small, that the temperature at all points of the cross section may be taken to be the same. The problem is thus one of one dimensional flow.

The rate of loss of heat from each element on the surface of the rod is proposed to be proportional to the temperature difference between the element and the environment. The latter temperature is constant. Assume, that the rod has a constant area of cross section A, the perimeter p and the surface conductance H. Further, let the ambient temperature be U_0. Then the rate $Q = Q(x)$, at which heat is lost by transmission at the surface per unit volume per unit time, is

$$Q = \frac{Hp(U - U_0)}{A} \qquad (4.2.1)$$

where $U = U(x)$ is the temperature of the rod at the point x. The rod is supposed to be covered by an insulation and be of length ℓ.

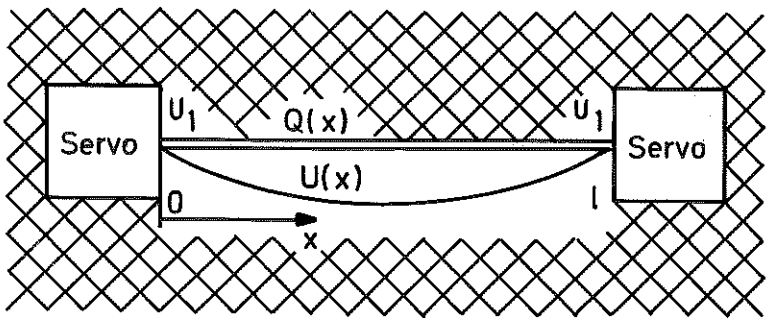

Fig. 4.2.1 - The rod and the servo covered by a conventional insulation.

Neglecting the dependence on temperature of the conductivity k, the specific heat c and the density ρ, the differential equation of conduction of heat in the rod can be obtained from eq. (4.1.3). We find

$$\partial^2 U/\partial x^2 - \frac{\rho c}{k}\,\partial U/\partial t = \frac{Hp(U - U_0)}{kA} \qquad (4.2.2)$$

Taking U_0 as the zero of the temperature scale, this equation becomes

$$\partial^2 u/\partial x^2 - \frac{\rho c}{k}\,\partial u/\partial t = \frac{Hpu}{kA} \qquad (4.2.3)$$

where

$$u(x) = U(x) - U_0 \qquad (4.2.4)$$

In the steady case we find

$$d^2u/dx^2 = \frac{Hpu}{kA} \qquad (4.2.5)$$

If the end surfaces of the rod are maintained at constant temperature U_1 and we put

$$\mu^2 = \frac{Hp}{kA} \qquad (4.2.6)$$

eq. (4.2.5) becomes

$$\begin{cases} d^2u/dx^2 - \mu^2 u = 0 & 0 < x < \ell \\ u = u_1 = U_1 - U_0 & x = 0 \\ u = u_1 = U_1 - U_0 & x = \ell \end{cases} \qquad (4.2.7)$$

The solution of eq. (4.2.7) is given by

$$u(x) = \frac{\sinh \mu(\ell-x) + \sinh \mu x}{\sinh \mu \ell} u_1 \qquad (4.2.8)$$

A perfect insulation gives the constant temperature u_1 along the rod. The deviation $\Delta u(x)$ from this ideal temperature reaches its maximum at $x = \ell/2$, owing to the symmetry of the construction. Defining

$$\Delta u(x) = u(x) - u_1 \qquad (4.2.9)$$

we obtain

$$\Delta u(\ell/2) = \left(2 \frac{\sinh \frac{\mu \ell}{2}}{\sinh \mu \ell} - 1 \right) u_1 \qquad (4.2.10)$$

This temperature difference will be used as a measure of the influence of the environment upon the process. The expression contains a parameter μ, which is a function of the unknown surface conductance H.

Fourier's law may be applied to yield the rate of flow of heat q_0 into either end surfaces of the rod. The law implies

$$q_0 = kA\left(\frac{du}{dx}\right)_{x=0} = - kA\left(\frac{du}{dx}\right)_{x=\ell} = kA \frac{\mu(\cosh \mu\ell - 1)}{\sinh \mu \ell} u_1 \qquad (4.2.11)$$

If heat is supplied to one end of the rod at a known rate, eq. (4.2.11) offers a very favourable way to determine μ and hence H. Noting, that the lateral loss of heat q_ℓ from the rod is equal to the flow of heat, supplied at the end surfaces, we get

$$q_\ell = 2q_0 \qquad (4.2.12)$$

In practice μ is often small, so that the hyperbolic functions

in eq. (4.2.10) and (4.2.11) may be replaced by the first terms of their series expansions. Thereby very handy expressions are obtained, valid for $\mu\ell \ll 1$. We find

$$\Delta u(\ell/2) = -\frac{1}{8}\mu^2\ell^2 u_1; \qquad \mu\ell \ll 1 \qquad (4.2.13)$$

and

$$q_0 = \frac{1}{2} kA\, \mu^2 \ell u_1; \qquad \mu\ell \ll 1 \qquad (4.2.14)$$

A substitution of eq. (4.2.14) into (4.2.13) considering (4.2.12) yields

$$\Delta u(\ell/2) = -\frac{1}{8}\,\frac{\ell q_\ell}{kA}; \qquad \mu\ell \ll 1 \qquad (4.2.15)$$

Recalling that $u_1 = U_1 - U_0$ a substitution of eq. (4.2.6) into (4.2.14) considering (4.2.12) gives

$$q_\ell = Hp\ell(U_1 - U_0); \qquad \mu\ell \ll 1 \qquad (4.2.16)$$

Observing, that $p\ell$ denotes the total surface through which the flow q_ℓ is transmitted, we conclude, that H at a first approximation equals the over-all coefficient of heat transfer, referred to the surface $p\ell$. Denoting the total thermal resistance between the rod and the environment by R we have

$$q_\ell = \frac{U_1 - U_0}{R} \qquad (4.2.17)$$

according to the definition of R. Combining eq. (4.2.16) and (4.2.17) we obtain

$$H = \frac{1}{Rp\ell}; \qquad \mu\ell \ll 1 \qquad (4.2.18)$$

From this expression the surface conductance H may be determined. It is quite simple shown that eq. (4.2.18) for small values of the product $\mu\ell$ yields a surface conductance somewhat smaller than the one obtained in reality. The total thermal resistance R is the sum of the individual thermal resistances, i.e. the resistance R_1 of the insulation and the two contact resistances R_{11} and R_{22} . Thus

$$R = R_1 + R_{11} + R_{22} \qquad (4.2.19)$$

In the figure below the rod of radius r_1, surface S_1 and conductivity k_1 and the insulation of radius r_2, surface S_2 and conductivity k_2 are shown. Denote the contact coefficient of the two boundary layers by h_1 and h_2. Then we have according to |1|

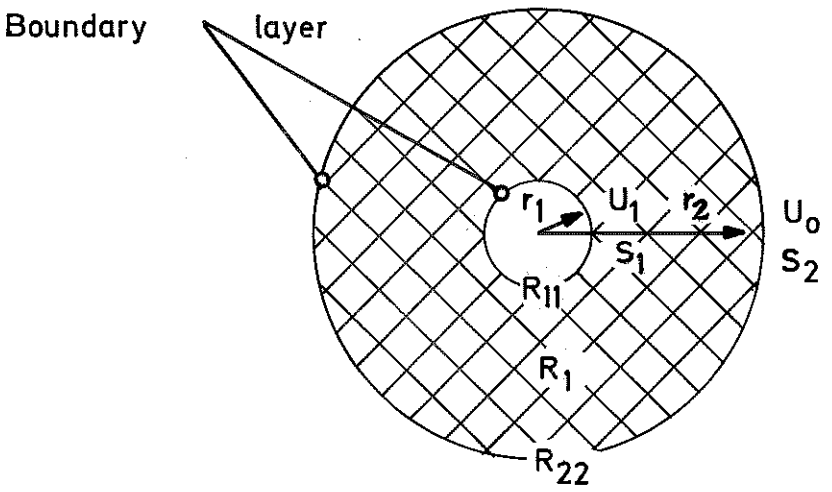

Fig. 4.2.2 - A crosscut of the rod and the insulation.

$$\begin{cases} R_1 = \dfrac{\ell n(r_2/r_1)}{2\Pi \ell k_1} \\ R_{11} = \dfrac{1}{h_1 S_1} \\ R_{22} = \dfrac{1}{h_2 S_2} \end{cases} \tag{4.2.20}$$

Let the dimensions of the rod and the insulation be given by

$$\begin{cases} r_1 = 0.70 \text{ cm} \\ S_1 = 2.0\ 10^2 \text{ cm}^2 \\ r_2 = 25 \text{ cm} \\ S_2 = 7.1\ 10^3 \text{ cm}^2 \\ \ell = 45 \text{ cm} \end{cases} \tag{4.2.21}$$

and put

$$\begin{cases} h_1 = h_2 = 5\ 10^{-4} \text{W/cm}^2\ ^{\circ}\text{C} \\ k_1 = 3.8 \text{ W/cm } ^{\circ}\text{C} \\ k_2 = 7\ 10^{-4} \text{W/cm } ^{\circ}\text{C} \end{cases} \tag{4.2.22}$$

The low values of the contact coefficients are obtained on the assumption, that natural convection takes place in the boundary layers. The conductivity k_1 is the one for copper. The value of the conductivity k_2 is achieved by a high test insulation. An insertion of the parameter values in eq. (4.2.20) yields

$$\begin{cases} R_1 = 18^{\circ}\text{C/W} \\ R_{11} = 10^{\circ}\text{C/W} \\ R_{22} = 0.3^{\circ}\text{C/W} \end{cases} \tag{4.2.23}$$

Putting

$$\begin{cases} U_0 = 25^{\circ}C \\ U_1 = 30^{\circ}C \end{cases} \tag{4.2.24}$$

the loss of heat q_ℓ is given by eq. (4.2.16). We find

$$q_\ell = 0.18 \text{ W} \tag{4.2.25}$$

Provided, that $\mu\ell << 1$ the temperature difference $\Delta u(\ell/2)$ may be calculated from eq. (4.2.15). We have

$$\Delta u(\ell/2) = -0.19^{\circ}C \tag{4.2.26}$$

The factor $\mu\ell$ is $4.5\ 10^{-2}$. The maximum permitted influence of the environment is $0.02^{\circ}C$, according to the system requirement (i). Thus the temperature difference $\Delta u(\ell/2)$ must be reduced approximately 10 times. An analysis shows, that this is not possible as long as a conventional insulation technique is used.

The evaluation above is carried out under the assumption, that the loss of heat from each element on the surface of the rod is proportional to the temperature difference between the element and the environment. This assumption is justified, if the thermal radiation q_r from the rod, being proportional to the fourth power of temperature, is neglectable. An upper limit of the radiation is achieved by taking the insulation to be a black body. Denoting the emissivity of copper by ε we find

$$q_r = \sigma S_1 \varepsilon \left[(U_1 + T_{abs})^4 - (U_0 + T_{abs})^4 \right] \tag{4.2.26}$$

where σ is the Stefan-Bolzmann constant and $T_{abs} = 273.15^{\circ}C$. The emissivity of polished copper is

$$\varepsilon = 0.10 \tag{4.2.27}$$

An insertion of the parameter values show

$$q_r = 0.06 \text{ W} \qquad (4.2.28)$$

Hence the radiant heat transfer maximally reaches 33% of the conduction heat transfer. The radiant heat transfer will henceforth be neglected.

4.3. A Final Approach.

From the previous section it is clear, that any conventional insulation technique cannot be employed to solve the problem of insulation. Such a technique results in an excess of the specified limit of the influence of the environment. A vacuum technique may be utilized. The used technique is the one sometimes found in equipments used for determination of the conductivity of solids. The bar is enclosed in a heat shield. In an ideal case the shield should be controlled so, that the temperature difference between equidistantly situated points on the bar and the shield is kept at zero. Such an arrangement should, however, complicate the construction essentially. From the evaluation, presented below, it follows, that very satisfying results even can be achieved, despite that only the end surfaces of the bar and the shield are kept at the same temperature.

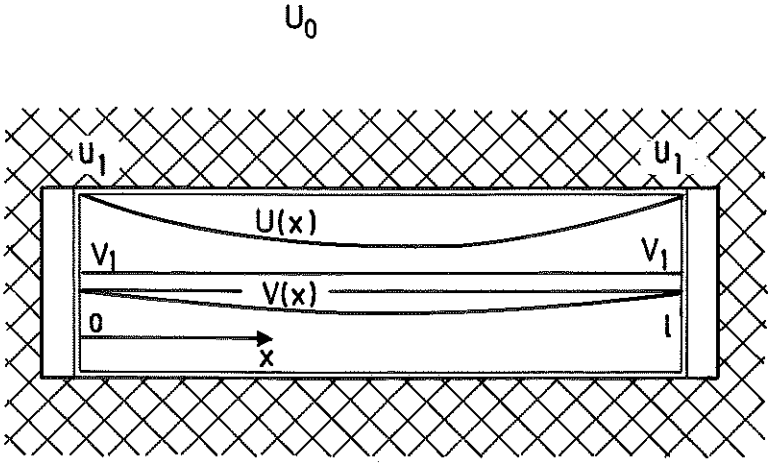

Fig. 4.3.1 - The bar enclosed in a heat shield.

The rest of this section will be devoted to the calculations of the bar temperature V(x) and the shield temperature U(x) in a case, where the end surfaces of the bar are maintained at the constant temperature V_1. In the evaluation we allow a temperature drop between the end surfaces of the bar and the shield. The end temperature of the shield is U_1. The bar and the shield are covered by a conventional insulation. The environment is air of constant temperature U_0. Further, the length of the bar and the shield is ℓ. The temperature profile V(x) gives a good measure of the quality of the construction. The heat flux from the bar is essentially less than the flux from the shield in any reasonable construction.

Assuming the loss of heat from each surface element to be proportional to the temperature difference between the element and its environment, the temperature U(x) can be obtained from eq. (4.2.4) and (4.2.8). Putting

$$\mu_2^2 = \frac{H_2 p_2}{k A_2} \tag{4.3.1}$$

where H_2 is the surface conductance, p_2 the perimeter, A_2 the cross section and k the conductivity of the shield, we find

$$U(x) = \frac{\sinh \mu_2(\ell - x) + \sinh \mu_2 x}{\sinh \mu_2 \ell} (U_1 - U_0) + U_0 \tag{4.3.2}$$

The calculation of the temperature V(x) is more involved as the temperature U(x) is not constant. The differential equation of conduction of heat in the bar can, however, be obtained from eq. (4.2.2). Denoting the conductivity k, the specific heat c, the density ρ, the surface conductance H_1, the perimeter p_1, and the cross section A_1 of the bar we have

$$\partial^2 V/\partial x^2 - \frac{\rho c}{k} \partial V/\partial t = \frac{H_1 p_1}{k A_1} \left(V - U(x)\right) \tag{4.3.3}$$

Putting

$$\mu_1^2 = \frac{H_1 p_1}{k A_1} \tag{4.3.4}$$

$$u_1 = U_1 - U_0 \tag{4.3.5}$$

and making the variable transformation

$$v(x) = V(x) - U_0 \tag{4.3.6}$$

eq. (4.3.3) becomes

$$\partial^2 v/\partial x^2 - \frac{\rho c}{k} \partial v/\partial t = \mu_1^2 \left[v - \frac{\sinh \mu_2(\ell-x) + \sinh \mu_2 x}{\sinh \mu_2 \ell} u_1 \right] \tag{4.3.7}$$

In the stationary case we find

$$\begin{cases} d^2v/dx^2 - \mu_1^2 v = -\mu_1^2 \dfrac{\sinh \mu_2(\ell-x) + \sinh \mu_2 x}{\sinh \mu_2 \ell} u_1 & 0 < x < \ell \\ v = v_1 = V_1 - U_0 & x = 0 \\ v = v_1 = V_1 - U_0 & x = \ell \end{cases} \tag{4.3.8}$$

The solution of eq. (4.3.8) is

$$v(x) = \frac{\sinh \mu_1(\ell-x) + \sinh \mu_1 x}{\sinh \mu_1 \ell} v_1 + \frac{\mu_1^2}{\mu_1^2 - \mu_2^2} \cdot$$

$$\cdot \left[\frac{\sinh \mu_2(\ell-x) + \sinh \mu_2 x}{\sinh \mu_2 \ell} - \frac{\sinh \mu_1(\ell-x) + \sinh \mu_1 x}{\sinh \mu_1 \ell} \right] u_1 \tag{4.3.9}$$

From this equation it can be seen, that $v(x)$ tends to the constant value v_1, as μ_1 and μ_2 tend to zero, i.e. as the insulation becomes perfect. Let the deviation $\Delta v(x)$ from the ideal temperature v_1 be defined by

$$\Delta v(x) = v(x) - v_1 \tag{4.3.10}$$

Owing to the symmetry of the construction, the deviation Δv reaches its maximum at $x = \ell/2$. A serie expansion of eq. (4.3.9) yields

$$\Delta v(\ell/2) = -\frac{1}{8}\mu_1^2\ell^2(v_1 - u_1) + \frac{5}{384}\mu_1^4\ell^4(v_1 - u_1) -$$

$$-\frac{5}{384}\mu_1^2\mu_2^2\ell^4 u_1 \qquad \mu_1\ell \ll 1,\ \mu_2\ell \ll 1 \tag{4.3.11}$$

This expression shows, that if a perfect thermal contact is obtained between the end surfaces, i.e. $U_1 = V_1$, the temperature difference $\Delta v(\ell/2)$ will be proportional to the fourth power of $\mu\ell$. In practice there will always be a small temperature drop between the two end surfaces. From the next section it follows, that the relation below approximately holds

$$V_1 - U_1 = v_1 - u_1 \leq 0.04^{\circ}C \tag{4.3.12}$$

at an ambient temperature $25^{\circ}C$.

Before the temperature differences $\Delta u(\ell/2)$ and $\Delta v(\ell/2)$ can be calculated all data of the construction must be available. The radius r_1, the surface S_1, the contact coefficient h_1 of the bar, the radius r_2, the surface S_2, the thickness d_2, the contact coefficient h_2 of the shield and the radius r_3, the surface S_3, the conductivity k_0, the contact coefficient h_3 of the outer insulation are given in the specification below. Here also the conductivities k and k_i of the bar and shield and the inner insulation respectively and the length ℓ appears.

$$\begin{cases} r_1 = 0.70 \text{ cm} \\ S_1 = 2.0\ 10^2 \text{ cm}^2 \\ r_2 = 2.7 \text{ cm} \\ S_2 = 7.6\ 10^2 \text{ cm}^2 \\ d_2 = 0.15 \text{ cm} \\ r_3 = 13 \text{ cm} \\ S_3 = 3.7\ 10^3 \text{ cm}^2 \\ \ell = 45 \text{ cm} \\ h_1 = h_2 = h_3 = 5\ 10^{-4} \text{ W/cm}^2\ ^{\circ}\text{C} \\ k = 3.8 \text{ W/cm } ^{\circ}\text{C} \\ k_i = k_0 = 7\ 10^{-4} \text{ W/cm } ^{\circ}\text{C} \end{cases} \tag{4.3.13}$$

From this specification the thermal resistances $\overset{0}{R}_1$, $\overset{0}{R}_{11}$, and $\overset{0}{R}_{22}$ of the outer insulation may be calculated. Eq. (4.2.20) yields

$$\begin{cases} \overset{0}{R}_1 = 7.9^{\circ}\text{C/W} \\ \overset{0}{R}_{11} = 2.6^{\circ}\text{C/W} \\ \overset{0}{R}_{22} = 0.5^{\circ}\text{C/W} \end{cases} \tag{4.3.14}$$

Putting

$$\begin{cases} U_0 = 25^{\circ}\text{C} \\ U_1 = 30^{\circ}\text{C} \end{cases} \tag{4.3.15}$$

and taking $\mu_2 \ell << 1$ the loss of heat q_2 and the surface conductance H_2 of the shield are according to eq. (4.2.16) and (4.2.18) given by

$$q_2 = 0.45 \text{ W} \tag{4.3.16}$$

$$H_2 = 1.2\ 10^{-4} \text{ W/cm}^2\ ^{\circ}\text{C} \tag{4.3.17}$$

Observing, that the cross section A_2 of the shield is equal to

$$A_2 = 2\pi r_2 d_2 \tag{4.3.18}$$

the coefficient μ_2 and the temperature difference $\Delta u(\ell/2)$ may be found from eq. (4.3.1) and (4.2.13). We get

$$\mu_2 = 1.4\ 10^{-2}\ 1/cm \tag{4.3.19}$$

$$\Delta u(\ell/2) = -0.26^{\circ}C \tag{4.3.20}$$

considering $\mu_2 \ell << 1$.

The factor $\mu_2 \ell$ is 0.65.

It now remains to determine the difference $\Delta v(\ell/2)$. This cannot be done until the coefficient μ_1, which is a function of the unknown surface conductance H_1, is known. It is immediately clear, that an upper limit of H_1 is the value of the contact coefficient obtained in a layer of air, where natural convection takes place, i.e. approximately $5\ 10^{-4}$ W/cm^2 $^{\circ}$C.

From specification (4.3.13) the resistances R_1^i, R_{11}^i, and R_{22}^i of the inner insulation may be obtained. We get

$$\begin{cases} R_1^i = 7.1^{\circ}C/W \\ R_{11}^i = 12^{\circ}C/W \\ R_{22}^i = 2.6^{\circ}C/W \end{cases} \tag{4.3.21}$$

Hence the total resistance R_i is

$$R_i = 21^{\circ}C/W \tag{4.3.22}$$

and according to eq. (4.2.18) the surface conductance H_1 is

$$H_1 = 2.4\ 10^{-4}\ W/cm^2\ ^{\circ}C \tag{4.3.23}$$

taking $\mu_1 \ell << 1$. An approximation of the loss of heat q_1 from the

bar may be obtained by employing eq. (4.2.17), where the temperature difference $U_1 - U_0$ is put equal to the mean temperature difference between the bar and the shield, i.e. $V_1 - U_1 - \frac{1}{2}\Delta u(\ell/2)$. We get

$$q_1 = 0.90\ 10^{-2}\ W \qquad (4.3.24)$$

Eq. (4.3.4), (4.3.13) and (4.3.23) yield

$$\mu_1 = 1.3\ 10^{-2}\ 1/cm \qquad (4.3.25)$$

Hence the factor $\mu_1\ell$ is 0.61. Given, that $\mu_1\ell$ and $\mu_2\ell$ may be taken as much less than 1 eq. (4.3.11) finally yields

$$\Delta v(\ell/2) = -\ 0.01^{\circ}C \qquad (4.3.26)$$

The calculated temperature difference $\Delta v(\ell/2)$ is well within its specified limits.

4.4. End Surface Contact.

The insulation method, described in the previous section, requires that the end surfaces of the bar and the shield are kept at almost the same temperature. As only the end temperature of the bar is controlled the quality of the thermal contact between the two end surfaces must be high. A silver plate thermally connects the two surfaces. The choice of the thickness of the plate becomes a compromise between the requirements of a small temperature drop in the plate and a swift settlement of the temperature to a reference temperature change.

A calculation of the temperature drop in the plate follows below. The same case is discussed as in the previous section, i.e. the end temperatures of the bar are 30°C and the ambient temperature is 25°C. From the previous section it follows, that the flow of heat into the bar may be neglected compared with the flow into

the shield. Consider a circular silver plate of radius R and thickness d connected to Peltier elements so that a constant effect per unit volume is generated in the plate.

Denote the total effect, emitted from the elements by q_0. The heat Q, supplied to the plate per unit volume per unit time, is

$$Q = \frac{q_0}{\pi R^2 d} \tag{4.4.1}$$

Neglecting the variation of the thermal properties of silver with temperature, the temperature distribution in the plate may be obtained from eq. (4.1.3) by means of a transformation of coordinates. In a cylindrical coordinate system we find in the steady state

$$\frac{1}{r}\frac{d}{dr}\left(r\frac{dU}{dr}\right) = -\frac{q_0}{\pi R^2 dk} \tag{4.4.2}$$

where $U = U(r)$ is the temperature in the plate at the radius r. An integration of eq. (4.4.2) from $r = 0$ to $r = r$ yields

$$\frac{dU}{dr} = -\frac{q_0}{2\pi R^2 dk}\, r \tag{4.4.3}$$

A second integration between the same limits yields

$$U(r) - U(0) = -\frac{q_0}{4\pi R^2 dk}\, r^2 \tag{4.4.4}$$

Consequently the searched temperature drop $U(R) - U(0)$ is

$$U(R) - U(0) = -\frac{q_0}{4\pi dk} \tag{4.4.5}$$

The flow of heat q_0 into the shield is given by eq. (4.3.16). The thickness d and the conductivity k of the plate appears in the specification below.

$$d = 0.20 \text{ cm} \tag{4.4.6}$$

$$k = 4.2 \text{ W/cm } ^{\circ}C \tag{4.4.7}$$

Using these values we find

$$U(0) - U(R) = 0.04^{\circ}C \tag{4.4.8}$$

The temperature difference is acceptable. The silver plate, used in the constructed process, is quadratic, a fact that does not affect the results appreciably. The connection of the cooler, the Peltier elements, the plate, the bar, and the shield are shown in full-size in the figure below.

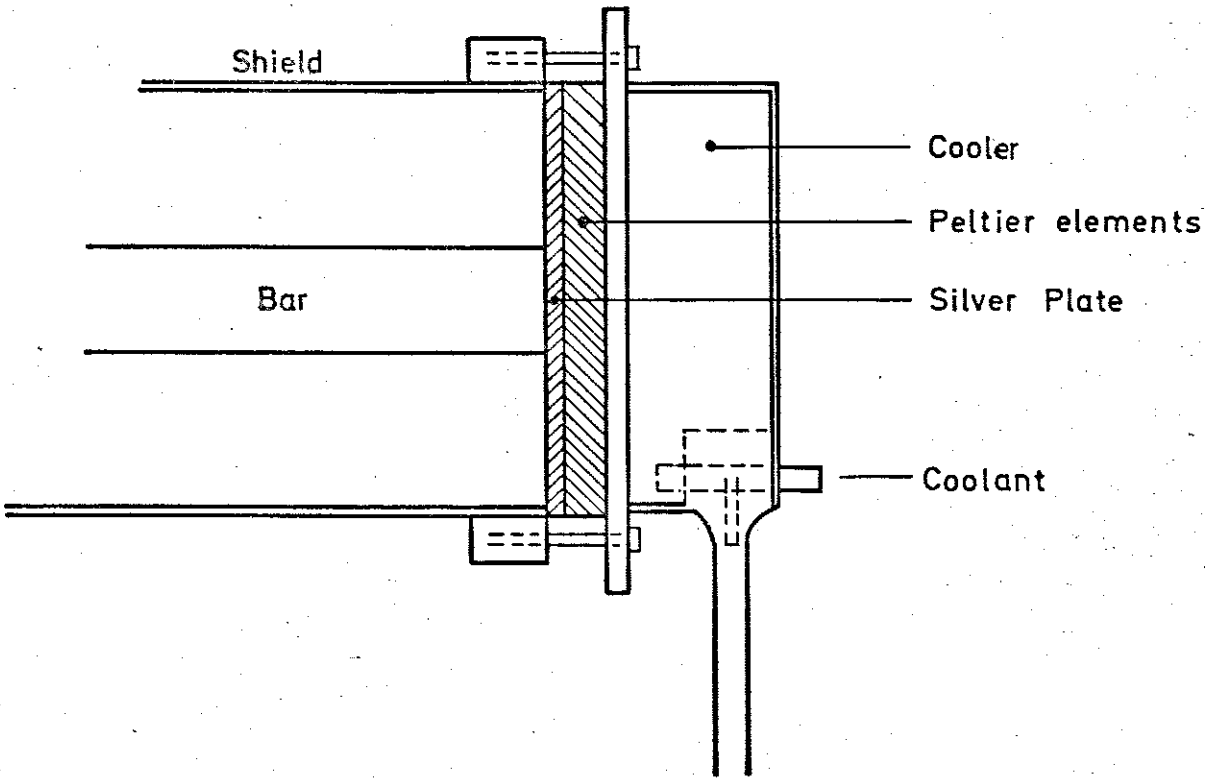

Fig. 4.4.2 - A full-size figure of the connection of the cooler, the Peltier elements and the plate.

Finally it is mentioned, that all basic equations involved in this chapter may be found in |1|.

5. FUNDAMENTALS OF THE DYNAMICS OF THE SYSTEM AND MEASUREMENT RESULTS.

5.1. Dynamics of the System.

Under ideal conditions the constructed process is described by the partial differential equation

$$\partial^2 U/\partial x^2 - \frac{1}{a^2}\,\partial U/\partial t = 0 \qquad (5.1.1)$$

The variable $U = U(x,t)$ denotes the temperature in a point x of the rod at time t.

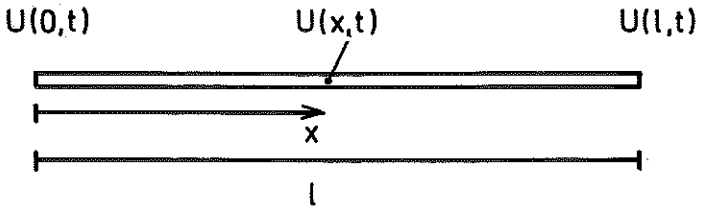

Fig. 5.1.1 - The ideal rod.

The diffusivity constant of the solid is denoted a^2. We have

$$a^2 = k/\rho c \qquad (5.1.2)$$

The quantities k, ρ, and c are the thermal conductivity, the density and the specific heat respectively of the rod. The length of the rod is ℓ. The variable transformation

$$t' = t/\tau;\ \tau = \ell^2/a^2 \qquad (5.1.3)$$

transforms eq. (5.1.1) into

$$\partial^2 u/\partial x^2 - \frac{1}{\ell^2}\,\partial u/\partial t' = 0 \qquad (5.1.4)$$

where $u = u(x,t')$.

The equation does not contain any material constants explicitely and turns out to be somewhat simpler to handle than the original equation. Of obvious reason τ is mentioned the time scale factor. The initial and boundary conditions of eq. (5.1.4) are

$$u(x,0) = 0 \qquad \forall x \tag{5.1.5}$$

$$\begin{cases} u(0,t') = u_1(t') \\ u(\ell,t') = u_2(t') \end{cases} \tag{5.1.6}$$

Introduce

$$\begin{cases} \mathfrak{L}\left(u(x,t')\right) = \theta(x,s') \\ \mathfrak{L}\left(u_1(t')\right) = \theta_1(s') \\ \mathfrak{L}\left(u_2(t')\right) = \theta_2(s') \end{cases} \tag{5.1.7}$$

where $\mathfrak{L}$ is the Laplace operator. Eq. (5.1.4) may be transformed into an ordinary differential equation by a Laplace transformation. Considering the initial condition (5.1.5) we find

$$d^2\theta/dx^2 - \frac{s'}{\ell^2}\,\theta = 0 \tag{5.1.8}$$

The boundary conditions of eq. (5.1.8) are

$$\begin{cases} \theta(0,s') = \theta_1(s') \\ \theta(\ell,s') = \theta_2(s') \end{cases} \tag{5.1.9}$$

The solution of eq. (5.1.8) with the boundary conditions (5.1.9) is

$$\theta(x,s') = \frac{\sinh \frac{\ell-x}{\ell}\sqrt{s'}}{\sinh \sqrt{s'}}\,\theta_1(s') + \frac{\sinh \frac{x}{\ell}\sqrt{s'}}{\sinh \sqrt{s'}}\,\theta_2(s') \tag{5.1.10}$$

Hence the transfer function (time t') between the temperature at a point x of the rod and the left end temperature is

$$G'(x,s') = \frac{\sinh \frac{\ell-x}{\ell} \sqrt{s'}}{\sinh \sqrt{s'}} \tag{5.1.11}$$

A modal analysis shows, that this transfer function may be written

$$G'(x,s') = 2\Pi \sum_{k=1}^{\infty} (-1)^{k+1} k \frac{\sin \frac{\ell-x}{\ell} \Pi k}{s' + \Pi^2 k^2} \qquad 0 < x \leq \ell \tag{5.1.12}$$

Transforming eq. (5.1.12) back to time t we find that the transfer function between the temperature at a point x of the rod and the end temperature is

$$G(x,s) = 2\Pi \sum_{k=1}^{\infty} (-1)^{k+1} k \frac{1}{\tau} \frac{\sin \frac{\ell-x}{\ell} \Pi k}{s + \frac{\Pi^2 k^2}{\tau}} \tag{5.1.13}$$

The transfer function contains an infinite number of negative real poles

$$s_k = - \Pi^2 k^2 / \tau \qquad k \neq k_i \tag{5.1.14}$$

The integers k_i are the integers, satisfying

$$\sin\left(\frac{\ell-x}{\ell} \Pi k_i\right) \neq 0 \tag{5.1.15}$$

At an irrational point x there does not exist any integers k_i, satisfying eq. (5.1.15). Note, that the poles s_k do not depend on the position of the point x.

The time constants T_k, corresponding to the poles s_k, are

$$T_k = \tau/(\Pi^2 k^2) \qquad k \neq k_i \qquad (5.1.16)$$

A 45 cm long copper rod yields

$$T_k = 188/k^2 \text{ sec.}, \quad s_k = -0.53\ 10^{-2}\ k^2 \text{ rad/sec.}; \ k \neq k_i \qquad (5.1.17)$$

The negative real part of the control poles of the temperature servo is

$$\text{Re}\{s_{cp}\} = 0.60 \text{ rad/sec.} \qquad (5.1.18)$$

Hence at an irrational point x the transfer function (5.1.13) contains 10 poles to the right of the control poles of the servo. The location of the poles s_k and the control poles of the servo is shown in the complex frequency s plane below.

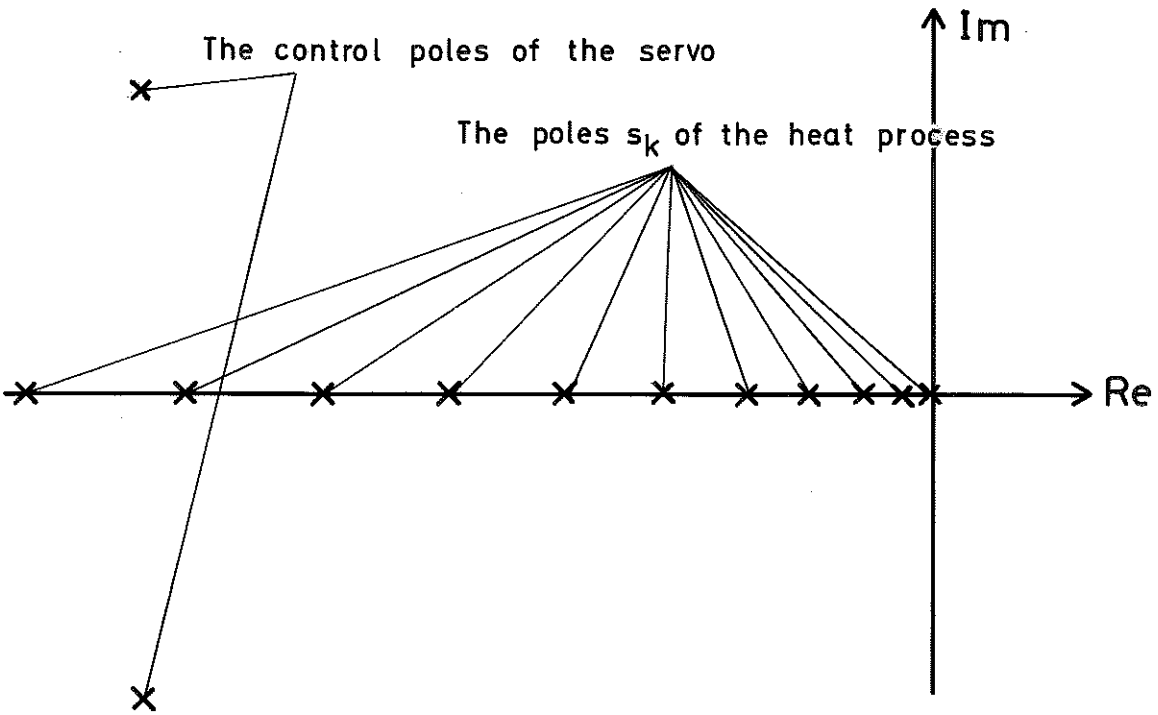

Fig. 5.1.2 - The location of the poles s_k of the one dimensional heat diffusion process and the control poles of the servo in a complex s plane.

At a rational point some of the marked poles are missing. The unit step responses v(x,t) at a point x can readily be calculated from eq. (5.1.13). We find

$$v(x,t) = \frac{\ell-x}{\ell} - \frac{2}{\pi} \sum_{k=1}^{\infty} (-1)^{k+1} \frac{\sin \frac{\ell-x}{\ell} \pi k}{k} e^{-\frac{\pi^2 k^2}{\tau} t} \qquad (5.1.19)$$

The formula is well suited for numerical calculations. The step responses v(x,t), for x = $\ell/8$, $2\ell/8$, ..., $7\ell/8$, are plotted in the Fig. 5.1.3. The time scale factor τ is chosen to 1.

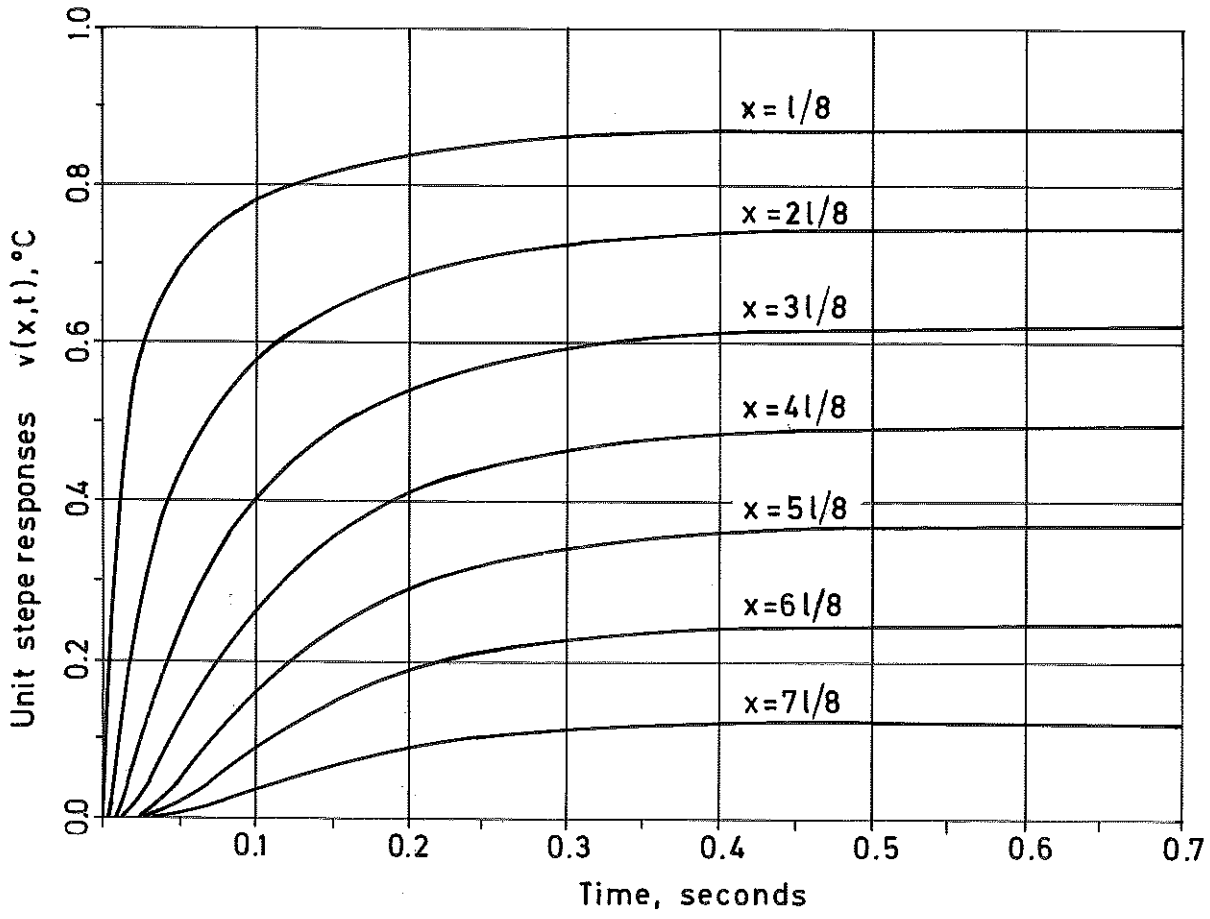

Fig. 5.1.3 - The unit step responses v(x,t) of the one dimensional heat diffusion process.

Eq. (5.1.19) implies, that the stationary temperature distribution in an ideal rod is linear.

5.2. Stationary Temperature Distribution of the System.

The measurement of the steady state temperature distribution of the system has been performed in two different cases. In the first case the end temperatures of the rod are kept equal and varied from 20°C to 30°C with the temperature increment 1°C. The measurement results are found in Table 5.2.1. The temperature errors $\Delta T = e_T - (T - T_0)$, $T_0 = 25^{\circ}C$, are calculated on the assumption, that the output of the transducers are related to the temperature T exactly by $e_T = T - T_0$, $T_0 = 25^{\circ}C$, in the range 20°C - 30°C. The table shows, that the registered temperature is somewhat too high for temperature below 25°C and somewhat too low for temperature above 25°C. The maximum temperature errors are obtained at the end points of the temperature range, i.e. at 20°C and 30°C. Approximately equal errors are obtained at the end points. These facts are stated by eq. (4.3.9). The maximum temperature error reaches 0.02°C. The postulated maximum error is 0.01°C according to eq. (4.3.26).

In the second case a temperature gradient is introduced in the rod. The different values of the end temperature of the rod are found in Table 5.2.2. The ideal profile for this case should be linear. The temperature errors $\Delta T = e_T - (T - T_0)$, $T_0 = 25^{\circ}C$, are evaluated under the same assumption as before. Note, that there is no longer a perfect correlation between the sign of the temperature errors ΔT and the sign of the output. This may be caused by the linearity error of the transducer. However, the maximum temperature error in Table 5.2.2 reaches 0.02°C. Thus the system requirement (i) is satisfied.

The stationary temperature difference between the mid point of the rod and the shield are measured in a case, where the end temperatures of the rod are kept at the constant temperature 30°C.

The difference reaches 0.30°C. The value agrees with the one given by eq. (4.3.20). The maximum temperature drop in the silver plate reaches 0.07°C.

All measurements have been performed with a digital voltmeter with the long term accuracy ±0.01% of full scale and ±0.02% of reading. The ambient temperature was 25°C.

Ambient temperature 25°C

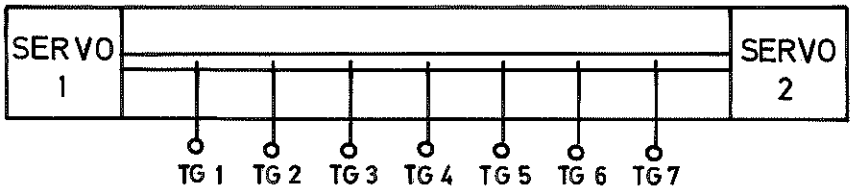

Output		Output							Temp. error $(e_T - (T-T_0))$						
S1	S2	TG1	TG2	TG3	TG4	TG5	TG6	TG7	TG1	TG2	TG3	TG4	TG5	TG6	TG7
V	V	V	V	V	V	V	V	V	°C	°C	°C	°C	°C	°C	°C
-5.000	-5.000	-4.992	-4.987	-4.986	-4.985	-4.978	-4.984	-4.982	0.008	0.013	0.014	0.015	0.022	0.016	0.018
-4.000	-4.000	-3.995	-3.991	-3.990	-3.988	-3.983	-3.988	-3.985	0.005	0.009	0.010	0.012	0.017	0.012	0.015
-3.000	-3.000	-2.998	-2.995	-2.995	-2.993	-2.987	-2.993	-2.990	0.002	0.005	0.005	0.007	0.013	0.007	0.010
-2.000	-2.000	-1.998	-1.998	-1.997	-1.996	-1.991	-1.996	-1.992	0.002	0.002	0.003	0.004	0.009	0.004	0.008
-1.000	-1.000	-1.001	-1.005	-1.005	-1.005	-0.998	-1.002	-0.999	-0.001	-0.005	-0.005	-0.005	0.002	-0.002	0.001
0.000	0.000	-0.003	-0.005	0.002	-0.002	-0.001	-0.001	-0.005	-0.003	-0.005	0.002	-0.002	-0.001	-0.001	-0.005
1.000	1.000	0.998	0.997	1.005	1.000	1.001	1.001	0.995	-0.002	-0.003	0.005	0.000	0.001	0.001	-0.005
2.000	2.000	1.991	1.989	1.990	1.994	1.996	1.996	1.992	-0.009	-0.011	-0.010	-0.006	-0.004	-0.004	-0.008
3.000	3.000	2.989	2.988	2.989	2.992	2.995	2.994	2.988	-0.011	-0.012	-0.011	-0.008	-0.005	-0.006	-0.012
4.000	4.000	3.988	3.985	3.987	3.991	3.993	3.993	3.985	-0.012	-0.015	-0.013	-0.009	-0.007	-0.007	-0.015
5.000	5.000	4.986	4.984	4.986	4.989	4.992	4.991	4.980	-0.014	-0.016	-0.014	-0.011	-0.008	-0.009	-0.020

Table 5.2.1 - The stationary temperature distribution of the rod (equal end point temperatures).

Ambient temperature 25°C

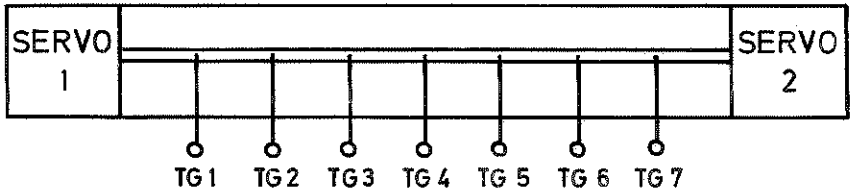

Output		Output							Temp. error $(e_T - (T-T_0))$						
S1 V	S2 V	TG1 V	TG2 V	TG3 V	TG4 V	TG5 V	TG6 V	TG7 V	TG1 °V	TG2 °C	TG3 °C	TG4 °C	TG5 °C	TG6 °C	TG7 °C
1.000	-5.000	0.246	-0.500	-1.259	-2.008	-2.759	-3.506	-4.242	-0.005	0.000	-0.009	-0.008	-0.009	-0.006	0.002
3.000	-5.000	1.995	1.000	-0.013	-1.011	-2.018	-3.013	-4.003	-0.005	0.000	-0.013	-0.011	-0.018	-0.013	-0.003
5.000	-5.000	3.750	2.503	1.248	-0.010	-1.273	-3.516	-3.758	0.000	0.003	-0.002	-0.010	-0.023	-0.016	-0.008
-5.000	1.000	-4.254	-3.510	-2.755	-2.002	-1.242	-0.495	0.248	-0.004	-0.010	-0.005	-0.002	0.008	0.005	-0.002
-5.000	3.000	-4.008	-3.018	-2.011	-1.008	0.005	1.002	1.997	-0.008	-0.018	-0.011	-0.008	0.005	0.002	-0.003
-5.000	5.000	-3.758	-2.522	-1.256	-0.010	1.255	2.504	3.746	-0.008	-0.022	-0.006	-0.010	0.005	0.004	-0.004
-1.000	5.000	-0.260	0.483	1.239	1.992	2.754	3.500	4.240	-0.010	-0.017	-0.011	-0.008	0.004	0.000	-0.010
-3.000	5.000	-2.009	-1.017	-0.008	0.994	2.009	3.005	3.993	-0.009	-0.017	-0.008	-0.006	0.009	0.005	-0.007
-5.000	5.000	-3.758	-2.522	-1.256	-0.010	1.255	2.504	3.746	-0.008	-0.022	-0.006	-0.010	0.005	0.004	-0.004
5.000	-1.000	4.247	3.494	2.740	1.991	1.237	0.488	-0.260	-0.003	-0.006	-0.010	-0.009	-0.013	-0.012	-0.010
5.000	-3.000	3.997	3.003	1.993	0.995	-0.013	-1.012	-2.004	-0.003	0.003	-0.007	-0.005	-0.013	-0.012	-0.004
5.000	-5.000	3.750	2.503	1.248	-0.010	-1.273	-2.516	-3.758	0.000	0.003	-0.002	-0.010	-0.023	-0.016	-0.008
-5.000	0.000	-4.377	-3.758	-3.126	2.500	-1.863	-1.243	-0.621	-0.002	-0.008	-0.001	0.000	-0.012	-0.007	-0.004
0.000	0.000	-0.003	-0.005	0.002	-0.002	-0.001	-0.001	-0.005	-0.003	-0.005	0.002	-0.002	-0.001	-0.001	-0.005
5.000	0.000	4.370	3.749	3.122	2.500	1.869	1.245	0.615	-0.005	-0.001	-0.003	0.000	-0.006	-0.005	-0.010
0.000	-5.000	-0.628	-1.252	-1.883	-2.504	-3.130	-3.752	-4.374	-0.003	-0.002	-0.008	-0.004	-0.005	-0.002	0.001
0.000	0.000	-0.003	-0.005	0.002	-0.002	-0.001	-0.001	-0.005	-0.003	-0.005	0.002	-0.002	-0.001	-0.001	-0.005
0.000	5.000	0.615	1.236	1.865	2.497	3.130	3.753	4.367	-0.010	-0.014	-0.010	-0.003	0.005	0.003	-0.008

Table 5.2.2 - The stationary temperature distribution of the rod (different end points temperatures).

5.3. Step Responses of the System.

The measurement of the step responses of the system has been performed with a data logger. A start command connects the input signals through ascending channel numbers to the digital voltmeter of the logger at each sampling period. The sampling period was 10 sec.

The step responses in the seven measuring points on the rod are recorded in three cases. In all cases one servo is kept at a constant temperature, 25°C, while an input step of approximately 1.8°C is applied to the other servo. The step is chosen so that the latter servo temperature remains in the range 24.1°C - 25.9°C. A negative input step first occurs. The responses $v_c(x,t)$; $x = \ell/8, 2\ell/8, \ldots, 7\ell/8$, are recorded until stationary conditions are achieved, which takes approximately 25 min. The responses $v_h(x,t)$; $x = \ell/8, 2\ell/8, \ldots, 7\ell/8$, to a positive input step of exactly the same magnitude as in the previous case, are then registered. The same steady state temperature distribution as initially obtained should now almost occur. The first described procedure is finally repeated. The recorded step responses are this time $v_c'(x,t)$, $x = \ell/8, 2\ell/8, \ldots, 7\ell/8$.

The linearity and stability of the step responses are checked by calculating the differences

$$DCH(x,t) = v_c(x,0) - v_c(x,t) - \left(v_h(x,t) - v_h(x,0)\right);$$

$$x = \ell/8, 2\ell/8, \ldots, 7\ell/8 \qquad (5.3.1)$$

$$DCC(x,t) = v_c(x,0) - v_c(x,t) - \left(v_c'(x,0) - v_c(x,t)\right);$$

$$x = \ell/8, 2\ell/8, \ldots, 7\ell/8 \qquad (5.3.2)$$

at each sampling event. The terms $v_c(x,0)$, $v_h(x,0)$, and $v_c'(x,0)$ accounts for the fact, that the output voltages do not equal zero at $t = 0$. In Fig. 5.3.1 the differences $DCH(x,t)$, $x = \ell/8, 2\ell/8, \ldots, 7\ell/8$, are shown.

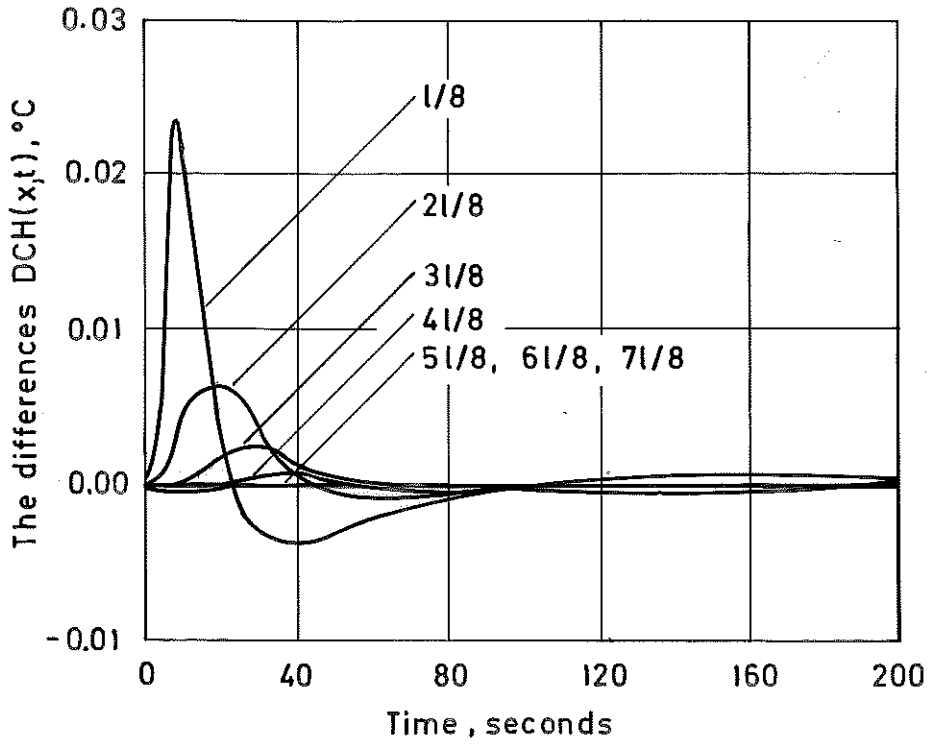

Fig. 5.3.1 - The differences DCH(x,t), $x = \ell/8, 2\ell/8, \ldots, 7\ell/8$, as a function of time t at an input temperature change of $1.8^{\circ}C$.

The spikes, appearing in the vicinity of origo, originate from the nonlinear components of the servo. For increasing x the spikes are decreasing or attenuated. The maximum differences DCH(x,t), $x \geq \ell/2$, are below $0.002^{\circ}C$. The differences DCC(x,t) are all within $0.002^{\circ}C$.

A measure of the deviation between the recorded step responses $v_c(x,t)$ and the theoretical responses $v_{th}(x,t)$ is given by

$$DMTH(x,t) = \frac{\ell-x}{\ell} \frac{v_c(x,0) - v_c(x,t)}{v_c(x,0) - v_c(x,\infty)} - v_{th}(x,t);$$

$$x = \ell/8, 2\ell/8, \ldots, 7\ell/8. \qquad (5.3.3)$$

The differences DMTH(x,t) are evaluated at each sampling event.

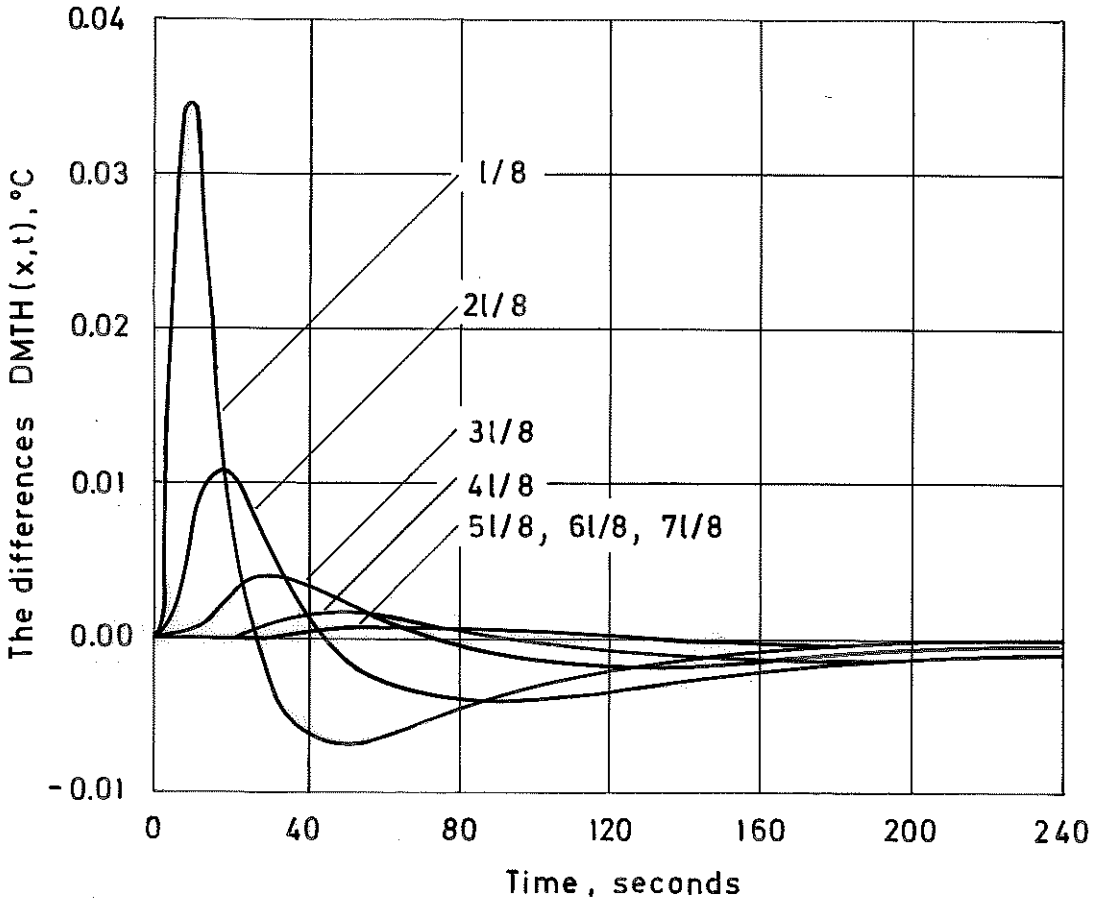

Fig. 5.3.2 - The differences DMTH(x,t), x = ℓ/8, 2ℓ/8, ..., 7ℓ/8 as a function of time t at a unit input step change.

Fig. 5.3.2 shows the differences DMTH(x,t) as a function of time. Note, that the measured responses are scaled before the evaluation of the differences DMTH(x,t) is performed. The spikes near origo are thus approximately twice as large when referred to the actual input step. The time scale factor τ, involved in the calculation of $v_{th}(x,t)$, is chosen so that an optimum fit (min-max criterion) between the responses is obtained. We find

τ = 1740

The theoretical scale factor is obtainable from eq. (5.1.3). We have

$$\tau_{th} = 1856$$

The discrepancy between the scale factors is caused by the dynamics of the servo. The theoretical calculations are performed on the assumption, that a perfect step is applied to the servo. Provided, that the length ℓ is known, the evaluation of the time scale factor τ is nothing but an evaluation of the diffusivity constant $k/\rho c$ of copper. The influence of the servo and the environment on the recorded responses maximally reaches $0.07^{\circ}C$. The value is obtained at the point $\ell/8$. As the measuring point is removed from the excitation point the influence is decreased and falls below $0.003^{\circ}C$ for $x \geq \ell/2$.

The employed data logger has a long term accuracy of $\pm 0.01\%$ of full scale and $\pm 0.02\%$ of reading. The variation of the length of the sampling period is kept within 0.1%. A perfect synchronism has been achieved between the start command of the logger and the change of input voltage to the servo. Corrections are made for the time displacement between the reading of the different channels within the same sampling period. The ambient temperature was $25^{\circ}C$.

6. ACKNOWLEDGEMENTS.

The author would like to express his gratitude to Lab.ing. H. Libelius, who did all the mechanical work.

7. REFERENCES.

|1| Mc Adams, W.: "Heat Transmission", Mc Graw-Hill.

|2| Carslaw, H.S., and Jaeger, J.C.: "Conduction of Heat in Solids", Oxford, 1959.

|3| Leden, B.: "Linear Temperature Scales from One Thermistor Reciprocal Networks", Report 7009, Oct., 1970, Lund Institute of Technology, Division of Automatic Control.

|4| Åström, E.: "Effektförstärkare med transistorer", Försvarets Forskningsanstalt, Report C 2281-54, 1968.

APPENDIX.

SYSTEM CONFIGURATION.

The system comprising of a heat process, a 19" modular rack, an interface to the digital computer PDP-15, a power control unit, a power amplifier, and a fan unit is shown in the Fig. A1.

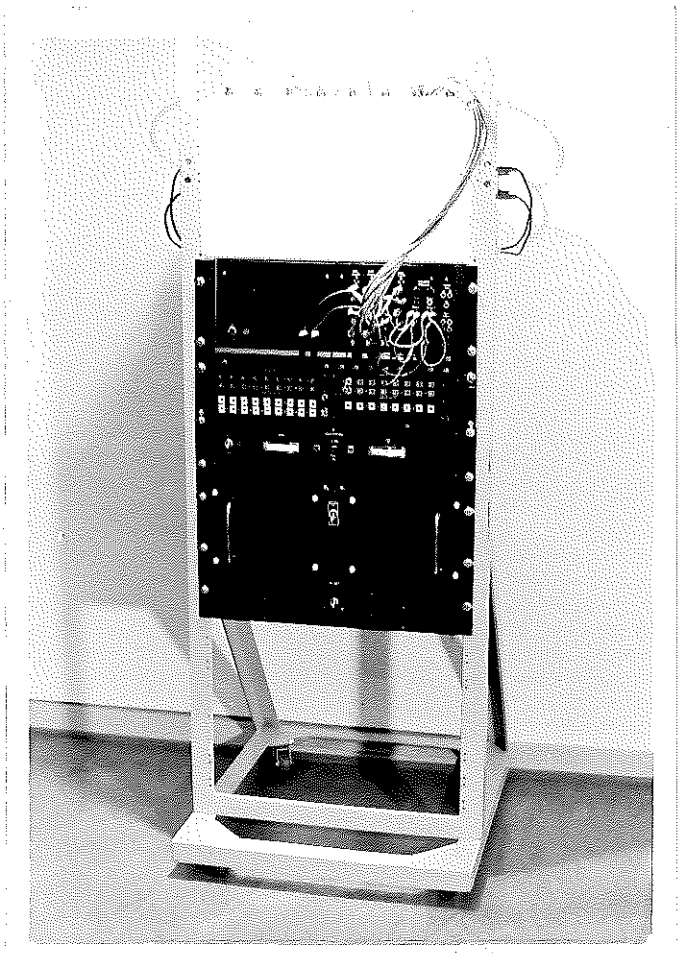

Fig. A1 - The system configuration.

The heat process, covered by a conventional heat insulation, appears in Fig. A2. The cooler, connected to the Peltier elements and the attachment of the 9 cables, containing the temperature sensors, may be studied from the picture.

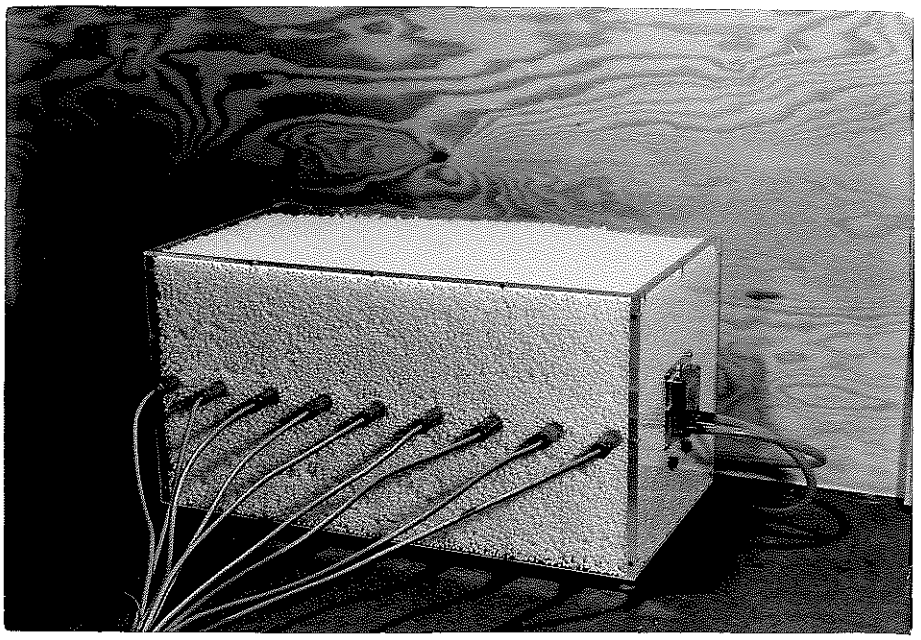

Fig. A2 - The heat process, covered by a conventional heat insulation.

All electronics, the power amplifier and the power control unit excluded, required to control and perform measurement on the heat process are contained in the 19" modular rack.

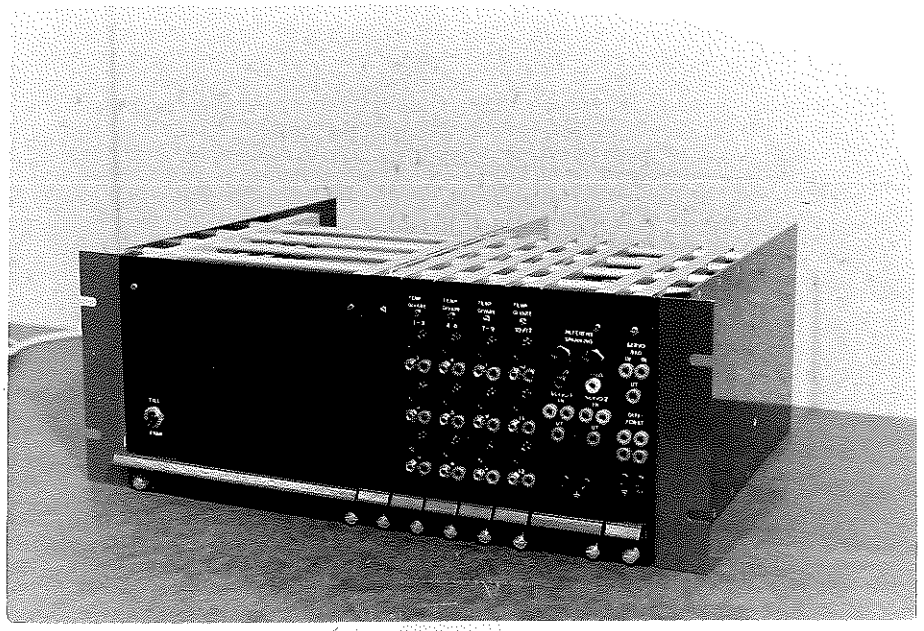

Fig. A3 - The 19" modular rack.

The rack comprises 8 modules. They are enumerated from the left to the right a 8" module, containing the supply voltage, a 1" module, containing the reference voltage feeding the bridges of the transducers, four 1" modules, containing the 12 temperature transducers, a 2" module, containing the summing amplifier and the compensation of the servo and finally a 1" module, containing among other things two differential amplifiers. Banana plugs are used to connect the different modules.